A STABLE-ISOTOPE INVESTIGATION OF VAPOR TRANSPORT DURING GROUND-WATER RECHARGE IN NEW MEXICO

By

Robert G. Knowlton, Jr.
Graduate Research Assistant

and

Fred M. Phillips
Principal Investigator

and

Andrew R. Campbell
Co-Principal Investigator

Geoscience Department, College Division
Geophysical Research Center, Research
and Development Division
New Mexico Institute of Mining and Technology

TECHNICAL COMPLETION REPORT

Project Number 1345644

February 1989

New Mexico Water Resources Research Institute

in cooperation with

Geoscience Department
New Mexico Institute of Mining and Technology

The research on which this report is based was financed in part by the U.S. Department of the Interior, Geological Survey, through the New Mexico Water Resources Research Institute.

DISCLAIMER

The purpose of Water Resources Research Institute technical reports is to provide a timely outlet for research results obtained on projects supported in whole or in part by the institute. Through these reports, we are promoting the free exchange of information and ideas and hope to stimulate thoughtful discussion and actions that may lead to resolution of water problems. The WRRI, through peer review of draft reports, attempts to substantiate the accuracy of information contained in its reports, but the views expressed are those of the authors and do not necessarily reflect those of the WRRI or its reviewers. Contents of this publication do not necessarily reflect the views and policies of the U.S. Department of the Interior, nor does mention of trade names or commercial products constitute their endorsement by the United States government.

ABSTRACT

New Mexico (especially the southern part of the state) is heavily dependent on ground water for agricultural irrigation, municipal supply, and economic development. The quantification of recharge is thus very important to scientists, engineers, and water resource planners.

We present a technique to model the transport of the stable isotopes ^{2}H and ^{18}O. This technique is based upon work by Barnes and Allison (1984). The model developed here can predict the shape of the stable isotope profiles in the vadose zone, and also quantify the vapor flux portion of soil-water movement. Through a non-linear least-squares approach, the model is matched to an observed isotope profile by optimizing the values of specified variables. The optimized parameters are then used to numerically solve for the vapor flux as a percentage of the deep flux of water below the root zone. This technique of modeling the isotope species transport is much more robust than conventional heat and moisture flow modeling techniques. This conclusion stems from the fact that the effective isotopic diffusivities vary little with water content, whereas hydraulic diffusivity is strongly dependent on water content.

Based upon the model results, in the top 2.7 meters of the soil profile a depth-averaged estimate of 15 to 33 percent of the total soil-water movement is in the vapor phase. This implies that the liquid flux of water is most important in the recharge process. However, the vapor flux is substantial enough to strongly influence the solute transport characteristics of the system. The strong downward vapor flux is also confirmed qualitatively by the pronounced minimum in the isotope profiles. The lighter isotopes, ^{16}O and ^{1}H, are preferentially transported in the vapor phase and condensed at depth, thereby causing the depletion of the isotope ratios.

A vacuum distillation procedure has been developed to extract soil water from soil samples without isotopic fractionation. This new technique is an alternative to the azeotropic toluene distillation method used by other investigators.

Key Words: stable isotopes, ground water, recharge, water vapor, deuterium, oxygen, tritium, chlorine

TABLE OF CONTENTS

LIST OF FIGURES

LIST OF FIGURES
(continued)

TABLE LISTING

ACKNOWLEDGMENTS

We would like to thank the staff of the Sevilleta National Wildlife Refuge for all their support and cooperation. Mr. Ted Stans has been especially helpful through the years of research done at the site.

INTRODUCTION

Ground water constitutes the sole water supply in much of New Mexico. Long-term availability of ground water is thus the primary limitation to economic development in many cases. This hydrologic reality has long been recognized by New Mexico water law through its control of ground-water withdrawal in basins which are threatened by overdraft. The goal of the legal regulation of pumping is to provide the maximum sustainable long-term water yield. This long-term yield is dependent not only on pumping rates, but also on the ground-water recharge rate. Knowledge of the recharge rate has important implications for the economic development of the state.

Many authors (e.g., Falconer et al. 1982; Mann 1976) have maintained that there is no direct recharge of ground water by infiltration of precipitation through the vadose zone of arid regions. Although this concept may be valid for some circumstances, localities exist in arid (and even hyperarid) environments which act as aquifer recharge areas due to incident precipitation (Verhagen et al. 1979; Dincer et al. 1974; Bergstrom and Aten 1965). The extent and importance of this type of recharge has probably been obscured due to misunderstanding of the behavior of soil

water in desert regions. Recent, detailed investigations in New Mexico (Stephens et al. 1985; Stephens and Knowlton 1986; Mattick et al. 1986; Phillips et al. 1988) have shown that direct recharge does take place in the arid portions of this state, and have shed light on the nature of the recharge process. Phillips et al. (1988) found that bomb-pulse chlorine-36, ^{36}Cl, and tritium, ^{3}H, have significantly different travel time characteristics in the vadose zone at two arid sites in New Mexico. They theorized that the movement of tritium was enhanced in the profile due to vapor transport. A solute such as ^{36}Cl would only travel in the liquid phase of water, and, therefore, would appear to be retarded with respect to the tritium movement. The downward movement of tritiated soil water appeared to be greater than twice the rate of the chlorine-36 movement at the study site. The soil-water movement in the upper portion of the profile is thus enhanced by a vapor phase flux of water. This vapor flux does not extend to the water table and contribute directly to recharge. The vapor flux does, however, enhance movement of soil water at shallower depths, thus contributing to the overall movement of soil water which eventually becomes recharge. Therefore, from a water resources planning perspective, vapor phase contributions to ground-water recharge may be important. Also, from a hazardous waste siting perspective, if vapor phase movement of soil water is significant, then volatile pollutants may

travel more rapidly through the vadose zone to an underlying aquifer than the dissolved constituents in the liquid-phase. Hence, non-volatile solutes may appear to be retarded relative to the movement of volatile constituents. Therefore, it may be important for engineers and water resource planners to quantify both the liquid and vapor flux in designing a hazardous waste facility.

This study uses the stable isotopes of hydrogen and oxygen, deuterium (^{2}H or D) and oxygen-18 (^{18}O), in the water molecule, to evaluate the relative importance of the vapor phase movement of water in the recharge process. A method to quantify the vapor phase contribution to soil-water movement is presented and appears to confirm the hypotheses presented by Phillips et al. (1988). It is expected that the enhanced understanding of the recharge process resulting from this research may allow more accurate estimation of ground-water recharge in New Mexico. It may also permit evaluation of methods for enhancing natural recharge in the state.

RELATED RESEARCH

Estimates of recharge rates in New Mexico under arid or semiarid conditions have been made by several investigators (Stephens et al. 1985; Stephens and Knowlton 1986; Mattick et al. 1986; Phillips et al. 1988). Stephens and Knowlton (1986) applied soil-physics techniques to quantify the amount of areal recharge through the vadose zone. They concluded that the recharge flux might be on the order of a few percent of the precipitation rate. This result is quite significant, considering that many previous studies in other arid environments have concluded that recharge is negligible. However, the soil-physics techniques employed in the Stephens and Knowlton (1986) study have statistical measurement errors as large as an order of magnitude.

Phillips et al. (1988) investigated the same site as that used by Stephens and Knowlton (1986). Phillips et al. (1988) used bomb-pulse ^{36}Cl and tritium as thirty year tracers for the estimation of water and conservative solute movement. One of their most interesting results was the relative positions of the bomb-^{36}Cl and bomb-tritium peaks in the soil profiles. Bomb ^{36}Cl and bomb tritium were both released by atmospheric nuclear weapons tests; the bomb-^{36}Cl

fallout peaking in about 1958 and the tritium fallout in 1964. The bomb ^{36}Cl was incorporated in precipitation and dry deposition and has been infiltrating slowly through the soil dissolved in the liquid soil water (Phillips et al. 1983; Phillips et al. 1984). The bomb tritium was incorporated into atmospheric water vapor (as the molecule HTO) and has also been moving downward with the soil water. If piston displacement is assumed, one would expect to find the bomb-tritium peak in the soil water at a slightly shallower depth than the bomb-^{36}Cl peak due to the timing of the fallout peaks. This has not proved to be the case.

Figure 1 shows the positions of the tritium and ^{36}Cl peaks for one soil profile measured at the Sevilleta National Wildlife Refuge, near Socorro. The bomb-^{36}Cl peak is found at a depth of about one meter, whereas the bomb-tritium peak is located at almost two meters. Thus, although the tritium entered the soil after the ^{36}Cl, it has penetrated deeper. Figure 1 also contains a graph of depth versus chloride age, based upon chloride mass-balance calculations. The chloride mass-balance appears to accurately predict the depth of the bomb-^{36}Cl peak. Limitations of the radio-isotope approach have been discussed by Phillips et al. (1988).

These results lead to the conclusion that tritiated water is moving downward faster than chloride. Two hypotheses offer likely explanations: (1) chloride is retarded relative to water by interaction with soil grains during

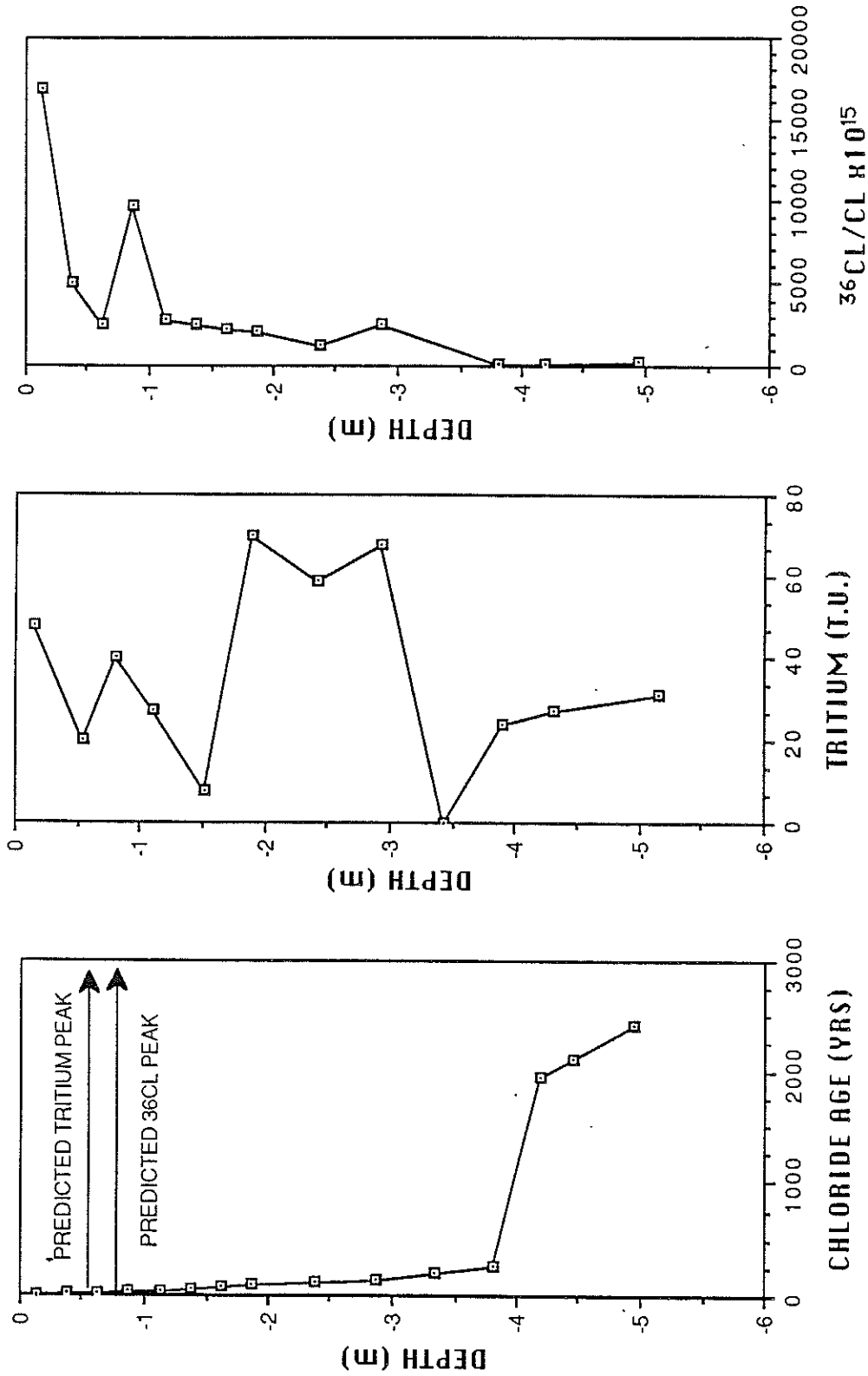

Figure 1. Predicted position of the bomb-^{36}Cl and ^{3}H peaks compared to the observed position. Chloride age is calculated by chloride mass balance method.(after Phillips et al.1988)

liquid flow, and (2) the tritium moves faster than the chloride because it is transported in both liquid and vapor phases whereas the chloride can travel only in the liquid phase.

Laboratory column experiments were devised by Mattick et al. (1986) to test the first hypothesis. The experimental conditions were designed so that only liquid flow of water and chloride was allowed and vapor transport was prevented by maintaining a zero vapor-pressure gradient. The chloride was observed to move relatively uniformly along with the moisture, indicating that the tracer had little chemical interaction with the porous media.

The second hypothesis is based on the fact that water (both H_2O and the isotopically labeled HTO) is volatile and can thus move as a gas, whereas chloride is not volatile and thus can be transported only when it is dissolved in liquid water. Net water vapor transport in the soil (due to gradients of partial pressure of water vapor) could, in turn, result from gradients of temperature, matric potential, osmotic potential, or a combination of these. Preliminary calculations suggest that average temperature and osmotic potential gradients are, by themselves, not sufficient to account for the observed difference between the ^{3}H and ^{36}Cl peaks. The matric potential gradients may work together with seasonally fluctuating temperature gradients to enhance downward vapor movement and restrict upward movement.

A recent laboratory study conducted by Grismer et al. (1986) has suggested that at low to moderate moisture contents the vapor-phase component of water flow may be significant. If the inferences made in Grismer's study, along with the radionuclide tracer work described above, are borne out, they will imply that in arid regions vapor-phase movement is at least as important as liquid-phase movement in transporting soil water below the root zone, where it can become groundwater recharge. In general, such a major role for vapor transport has not been previously recognized, and it has important implications for determining ground-water recharge in desert soils. Commonly-used soil-physics methods of measuring recharge, based on Darcy's law, normally only involve liquid-phase flux calculations. The often-used chloride mass-balance method (Stone and McGurk 1985) also accounts only for liquid flow. Thus, actual recharge amounts may be larger than those determined by these methods, by at least a factor of two.

Differentiation of liquid and vapor fluxes by standard physical measurements is quite difficult, due to the large variation of matric potential with water content at high soil-water suctions. This is not the case when applying direct tracing techniques using the stable isotopes of hydrogen and oxygen in the water molecule. This technique takes advantage of the fact that the diffusivities of the isotopic species vary little with water content (unlike

hydraulic conductivity) and the method is thus more robust at low water content than calculations based on Darcy's law (Barnes and Allison 1984).

The systematics of oxygen and hydrogen isotope variation in precipitation (Dansgaard 1964) have been understood for over twenty years. However, understanding of the isotopic systematics in soils has lagged considerably. The foundations were laid by Zimmerman et al. (1967). The basic mathematical formulations they developed are still used, however, they limited their theory and experiments to evaporation from saturated soils. More recent investigations in humid climates by Thoma et al. (1979), Bath et al. (1982), and Saxena (1984) have been able to apply the theory of Zimmerman et al. (1967) with little modification.

The much more difficult problem of isotope distribution in dry, desert soils was not addressed until the work of Allison (1982). Since then, this topic has been further treated by a formal theoretical description for isothermal soils (Barnes and Allison 1983), laboratory experiments involving dry soils (Allison et al. 1983), field investigations in a semiarid region (Allison and Hughes 1983), and a theoretical development for non-isothermal soils (Barnes and Allison 1984). The last citation is most pertinent to the study presented here, inasmuch as the theory allows for downward diffusion of water vapor under temperature gradients. This phenomenon may have been observed under labora-

tory and field conditions (Allison 1982; Bath et al. 1982; Allison and Hughes 1983), but these investigators were unable to analyze their results for non-isothermal conditions due to a lack of temperature data. Examples of the application of these stable-isotope techniques in field situations can be found in Allison et al. (1984) and Allison et al. (1985). Most of this previous work has concentrated on quantifying evaporation rates from the soil surface, and not the downward flux of vapor through the profile. Hence, our goals require an advance in the application of these techniques.

SITE DESCRIPTION

The field site comprises an area of about 1.3 square kilometers in the Sevilleta National Wildlife Refuge about 24 kilometers north of Socorro, NM (Figure 2). The site lies within the Rio Grande drainage basin on the south side of the Rio Salado, an ephemeral, braided tributary to the mainstream. The area receives about 20 cm of precipitation per year and the gross annual lake evaporation is about 178 cm (U.S. Department of Agriculture 1972).

The surficial geology has been mapped by Machette (1978), and consists mostly of fluvial sands and dune sand (Figure 3). A few discontinuous, thin silt and clay layers exist beneath parts of the area. Vegetation is relatively sparse, consisting of salt cedar along the ephemeral drainage, saltbush, creosote, juniper and grasses on the ancient flood plain, and only a few juniper near the edges of the sand dune. Greater vegetation density is suggested where a shallow low-permeable layer is beneath the sand-covered, ancient, flood plain. The predominant vegetation around our sampling locations are saltbush and grasses. Depth of saltbush rooting appears to be limited to the upper 1.0 to 1.5 meters (Stephens et al. 1985); however, quantification studies are needed. The topography varies from

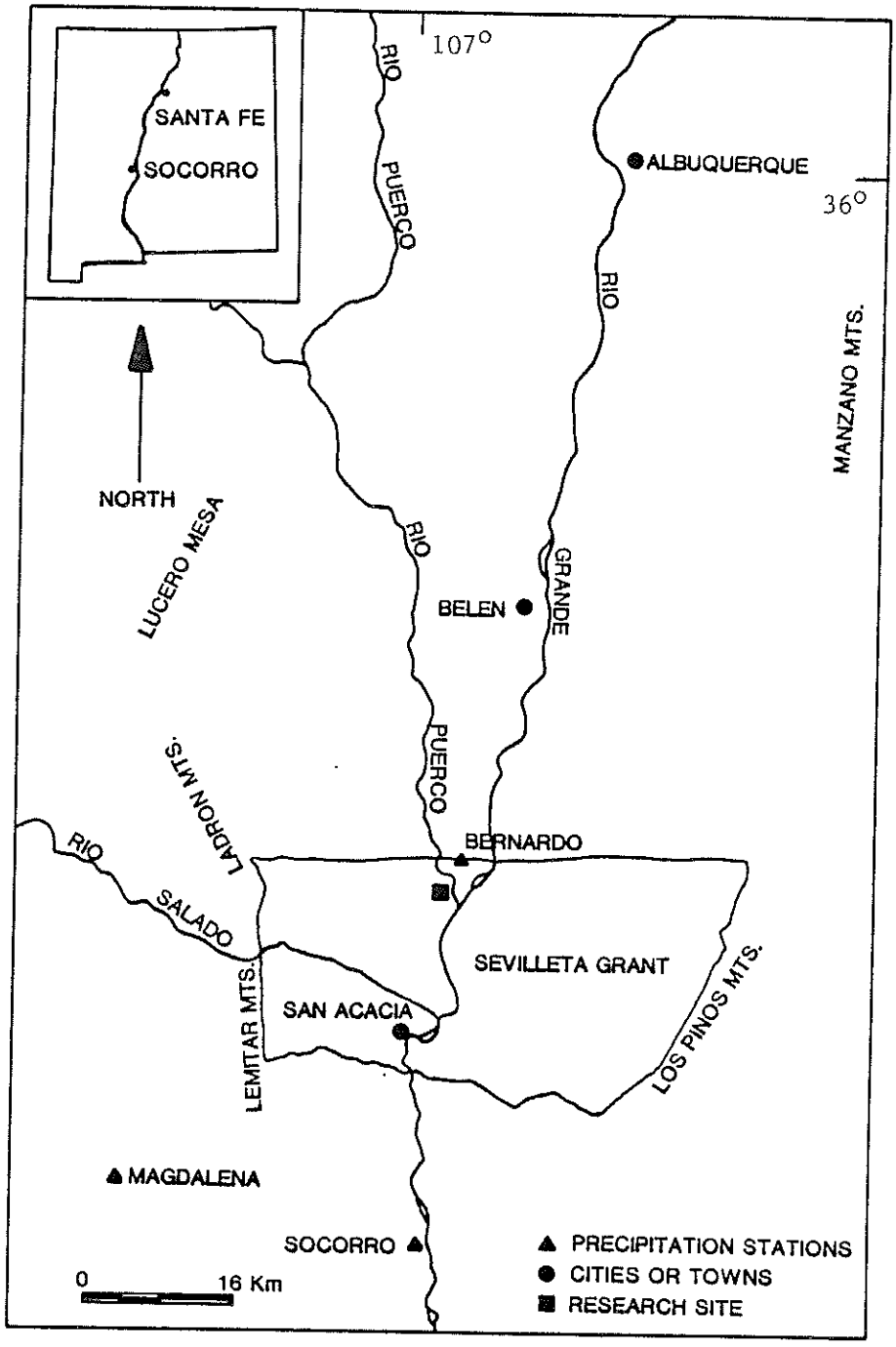

Figure 2. Site location map (after Stephens et al. 1985)

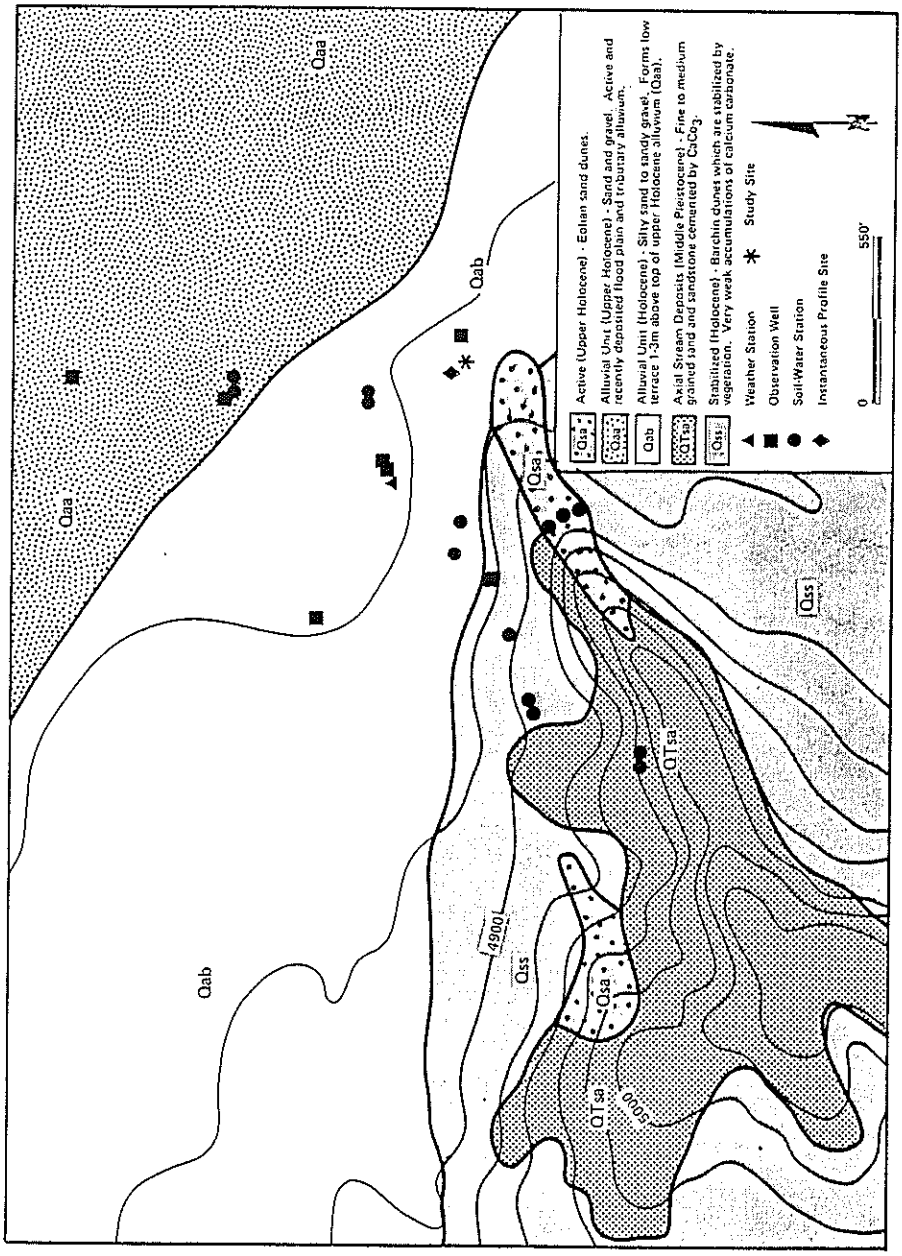

Figure 3. Instrument locations and geologic map, with topography contours in feet above mean sea level. (after Stephens et al. 1985)

moderate slopes near the sand dunes (Qsa) and sandstone outcrop (QTsa) to nearly flat lands on the ancestral flood plain (Qab).

In the lowland areas, the depth to less permeable Pleistocene sediments is about 17 meters and the depth to ground water is only about 3 meters. Near soil-moisture station 1 (see Stephens et al. 1985 for complete instrumentation description) the depth to ground water is approximately 6 meters. The aquifer consists mostly of unconsolidated sand with some cobbles. The hydraulic gradient is eastward in the direction of the grade of the Rio Salado channel.

No evidence of runoff from the sampling site has been observed since monitoring began in November 1982, based on field observations (Stephens et al. 1985). The Rio Salado flows mostly during August and September in response to intense thunderstorms in the mountains to the west. Approximately half of the annual rain and snow falls during the winter. Precipitation does not generate runoff, owing to the infiltration characteristics of the sandy surficial deposits (Stephens et al. 1985).

The monitoring network that exists at the site includes a weather station; a number of observation wells, some with continuous recorders; and fifteen soil-water monitoring stations. For a more detailed discussion of this instrumentation see Stephens et al. (1985). The radioisotope work conducted by Mattick et al. (1986) was done in close proximi-

ty to soil-moisture station 1. Work carried out in this study was also performed within 15 meters of this station. Of course, there is always the consideration of spatial and temporal variability, and the correlation of results from one site to another.

METHODS AND PROCEDURES

Field and Laboratory Methods

Field Sampling. Seven coreholes were drilled at the Sevilleta National Wildlife Refuge in the course of this study. Two methods were employed to obtain soil samples: rotary hollow-stem augering with a drill rig, and hand augering. The first two coreholes drilled at the site used a drill rig, a Mobile B-60, owned by the State of New Mexico, Environmental Improvement Division (NMEID). A continuous profile of soil samples was obtained from the coreholes by sampling with shelby tubes just ahead of the auger. The samples collected ranged from land surface to 5.0 meters in depth. The shelby tubes were sealed to prevent evaporation and transported back to the laboratory. In the laboratory these samples were sectioned immediately into smaller subintervals. The soil samples were then sealed in glass jars to prevent evaporation of the soil water. The jars were refrigerated to minimize any biological activity.

A hand augering technique was also used to obtain continuous soil sampling. Once the soil was removed from the corehole, the sample was immediately placed in a glass canning jar and sealed to prevent evaporation. At each depth interval sampled, a thermistor was lowered down the hole and temperature recorded for later use in numerical modeling.

Depth of sampling was generally from land surface to approximately 4.5 meters.

Distillation Techniques. Two techniques are now available for distilling soil water from a soil sample without appreciable isotopic fractionation. The two techniques are azeotropic toluene distillation and vacuum distillation. The first technique is discussed briefly by Allison et al. (1985).

Before beginning an azeotropic distillation, the soil sample must be split, one subsample used for distilling soil water, and the other to determine gravimetric water content. A special distillation apparatus is needed to perform the extraction. The soil sample is placed in a boiling flask and toluene is added until it just covers the top of the soil. The boiling flask is then connected to a condensing column, and a heating element set under the flask. The soil/toluene mixture is heated to just below the boiling temperature of water, < 100°C. The soil water and toluene form an azeotrope, and are boiled off and condensed without isotopic fractionation between 84 and 100°C (Kirk-Othmer 1983). Because there is no fractionation during the process, the technique does not require distillation of all the soil water. When the water/toluene mixture is condensed in the sidearm of the apparatus, the two constituents separate, but some residual dissolved toluene is left in the water. The water obtained from each sample is purified of any toluene

contamination by introducing paraffin wax into the sample and heating. The paraffin is supposed to absorb the dissolved toluene from the water. The paraffin wax then cools above the water in the sample bottle to form a seal. These sample bottles are then put in refrigerated storage until they can be analyzed. Through repeated experimentation it was found that the effectiveness of the paraffin in purging the sample of toluene was inadequate. The residual toluene contamination carried through the other gas preparation techniques, causing contamination in the mass spectrometric analyses. Therefore, an alternative method for distilling soil water was necessary.

The second method for distilling soil water was developed, tested, and evaluated for this project. The technique employs the use of a distillation line, liquid nitrogen, gaseous nitrogen, a heating element, and a vacuum pump. Figure 4 illustrates the distillation line setup schematically.

The vacuum distillation procedure consists of three steps. First, the soil water is frozen. Next, a vacuum is applied to the distillation line. Third, the soil water is boiled over to a collection flask cooled with liquid nitrogen. The distillation continues until all the water is extracted from the soil. A more detailed discussion of the procedures involved in this vacuum distillation technique follows.

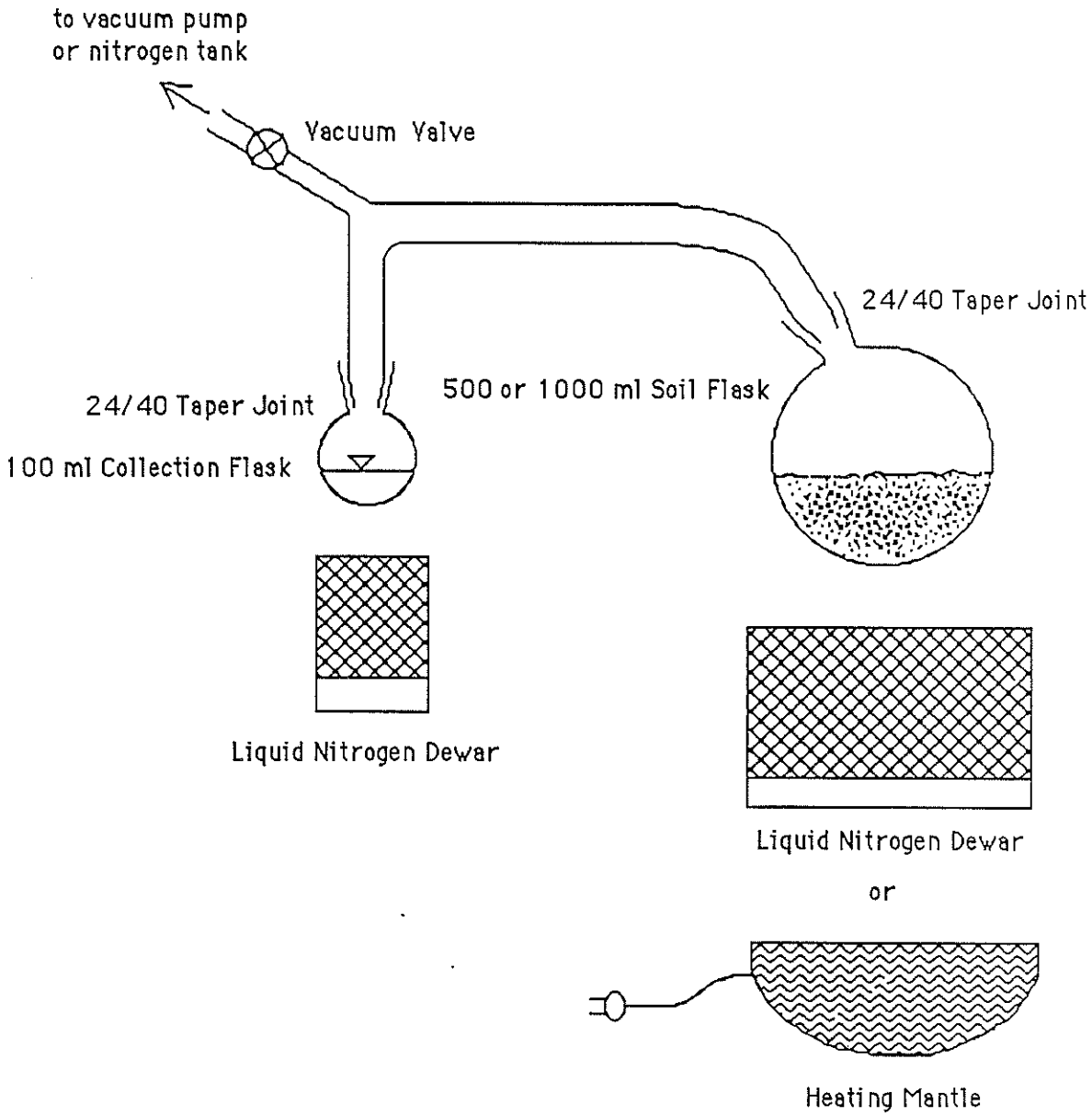

Figure 4. Vacuum distillation line schematic

In the first step, the glass flasks and the distillation line are purged of any atmospheric gases and water vapor by flooding with gaseous nitrogen from a compressed gas cylinder. This purging minimizes any potential atmospheric contaminants, such as CO_2 or water vapor, from entering the soil water. A soil sample is placed in the boiling/-freezing flask and the distillation line is assembled. With the distillation line completely sealed, a liquid nitrogen bath is placed around the soil flask. The soil water is frozen for a period of approximately 10 minutes.
Next, a vacuum line is attached and a vacuum pulled on the distillation line. All the residual gases are pumped from the system. The pressure is decreased to a vacuum pressure of 100-200 millitorr, which speeds the distillation process. The distillation line is again sealed, the liquid nitrogen taken away, and a heating element applied to the soil flask. A liquid nitrogen filled dewar is then placed around the capture vessel. The distillation of soil water from the soil flask to the capture vessel then proceeds under a diffusion/thermal gradient. This procedure may take several hours depending on the amount of soil water in the sample, and the soil texture. When all the soil water has been condensed into the capture flask, as evidenced by the cessation of condensation, the distillation line is flooded with gaseous nitrogen again. This step minimizes atmospheric contamination. The capture flask is removed and immediately capped.

If moisture contents were desired, the weighing of flasks before and after distillation facilitates that calculation, inasmuch as all the water is distilled from the soil. It is imperative that the soil water be stored in sealed sample bottles, with an additional paraffin seal around the top, to prevent any evaporation or contamination.

Some precautions must be taken to ensure proper distillation results. If the soil water yield is not within 99.75 to 100% of the total water in the subsample, there can be an appreciable amount of fractionation. Figure 5 illustrates the relationship between the change in isotopic composition of δ^2H and the residual fraction of water distilled, for several values of temperature. The curves were calculated using a simple Rayleigh distillation equation. A similar set of data could also be prepared for the change in $\delta^{18}O$ with residual fraction. In addition to adequate yield, if there is significant atmospheric contamination during the procedure, the isotopic composition of the water may change.

Another factor contributing to possible error is the method by which the soil-water samples are stored after distillation. The soil water is stored in glass jars with teflon caps. If the integrity of the seal is not maintained, the soil water may evaporate from the bottle. If the water sample stored in the bottle is small, and enough time elapses, fractionation has been observed to occur. Therefore, for soil water storage, a paraffin seal is formed

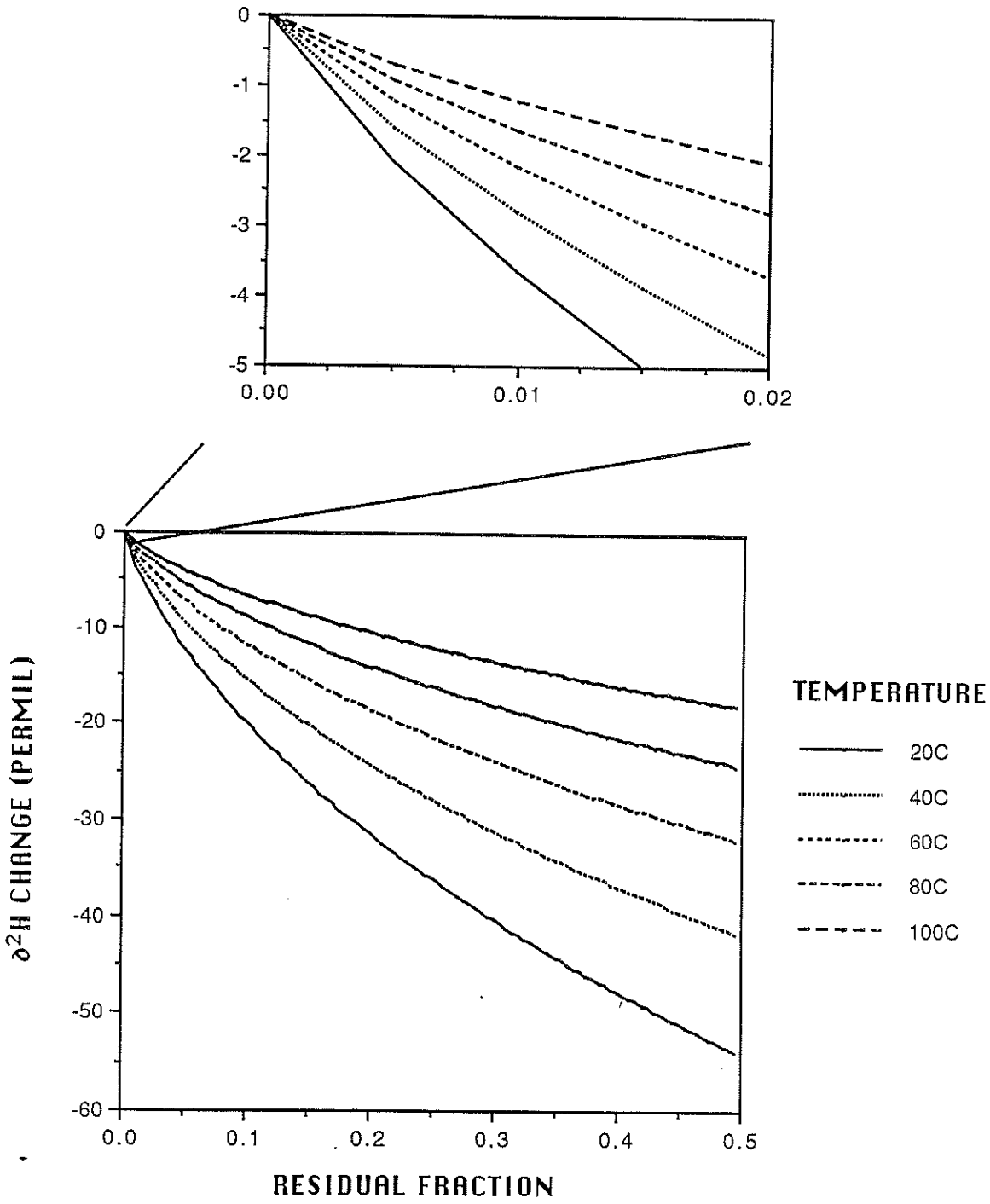

Figure 5. Change in δ^2H versus residual fraction of water left during the distillation process

around the outside of the bottle cap.

This vacuum distillation technique requires great care and more time than the toluene distillation method. However, due to the dissolved toluene contamination of the extracted soil water with the toluene distillation method, it is advantageous to use the vacuum distillation technique.

CO_2/H_2O Equilibration Technique. To analyze a water sample for its $^{18}O/^{16}O$ ratio, the water must be equilibrated with CO_2, and the CO_2 analyzed on a mass spectrometer. The CO_2/H_2O equilibration technique used in this study was not previously used at the New Mexico Institute of Mining and Technology Stable Isotope Laboratory. Therefore, the equilibration setup for this technique was constructed during this project.

The apparatus and procedures for this equilibration technique were outlined by Roether (1970). Roether's procedure is a variation of the standard technique employed by Epstein and Mayeda (1953). The technique involves equilibrating a CO_2 gas of known isotopic composition with the water sample of interest in a special glass equilibration vessel. Water volumes of 1 to 10 milliliters are generally applicable. The equilibration vessel is placed in a constant temperature shaker bath. This step is not included in the Epstein and Mayeda technique. The shaker bath must be capable of shaking at a frequency greater than the resonance frequency of water, about 3.8 cycles/sec, to optimize the

equilibration time. Typically, the frequency of the shaker bath is set at 5.0 cycles/sec. Equilibration times for the Roether technique are therefore on the order of 2 hours, as compared to several days with the Epstein and Mayeda technique. The equilibrated CO_2 gas is then purified and transferred to a sample bottle on an extraction line. That sample bottle is then mounted directly on the inlet system of the mass spectrometer for isotopic ratio analysis.

H_2 Reduction Technique. To determine the $^2H/H$ ratio of the water, a reduction technique must be employed to generate hydrogen gas from the water sample. A relatively newly developed zinc reduction technique has been set up for this project (Kendall and Coplen 1985).

The hydrogen reduction technique involves the heating of the soil water in a reaction vessel in the presence of zinc. Special reaction vessels and an aluminum block heater are needed, as outlined by Kendall and Coplen (1985). The zinc used in this reduction procedure must have special additives in order to reduce the water sample without fractionation. The altered zinc is considered to be 'optimally contaminated'. A sample of 'optimally contaminated' zinc, obtained from Indiana University, is placed in the bottom of a reaction vessel. Approximately 0.25 grams of zinc is used with a water sample of 5 microliters. At the start of the procedure, the vessel is sealed and pumped on by a high vacuum system. The zinc is heated with a heat gun to drive

off any adsorbed atmospheric water vapor. The vessel is attached to a special port on the line which allows the syringe injection of the water sample through a septum. A dewar of liquid nitrogen is placed around the base of the vessel, covering the zinc. When the water is injected into the apparatus, it is condensed down to the zinc. A heat gun is used to speed the transfer process. The vessel is then sealed and removed from the vacuum line. It is then placed in the aluminum block heater at a temperature of 500°C for 30 minutes. Almost immediately after entering the heater, zinc oxide and hydrogen gas are formed. The vessel is then ready for direct connection to the inlet system of the mass spectrometer for analysis.

Mass Spectrometry. Several laboratories have been employed to measure the isotopic compositions of the gases prepared from these soil samples. Samples have been run at Yale University, the U.S. Geological Survey Laboratory in Reston, VA, the University of Missouri at Columbia, the University of New Mexico, and recently at the New Mexico Institute of Mining and Technology. Disappointingly, problems with inter-laboratory calibrations, toluene contamination, early vacuum distillation procedures, and mass spectrometry analyses resulted in the exclusion of the data from labs other than the New Mexico Institute of Mining and Technology in the numerical analyses. These data did help to refine the preparation techniques so that the samples

analyzed at the New Mexico Institute of Mining and Technology were of good quality. Most of the ^{18}O and deuterium data reported here have been collected on the New Mexico Institute of Mining and Technology's Finnegan-MAT Delta E mass spectrometer. Analytical precision on the Delta E is ± 0.1 $^{o}/_{oo}$ (permil) for CO_2 and ± 0.5 $^{o}/_{oo}$ for hydrogen.

Numerical Modeling Methods

The main objective of this study was to estimate the relative contribution of the water vapor flux to soil-water movement. Phillips et al. (1988) have shown that bomb-pulse ^{36}Cl and ^{3}H have markedly different travel path/time characteristics. They attributed the discrepancy in peak depths for these two tracers to enhanced vapor phase movement of the tritium. Therefore, a technique for quantifying the vapor flux was needed.

A theoretical model for predicting the vapor flux of water during steady evaporation from a water table was developed by Barnes and Allison (1984), hereafter referred to as the 'non-isothermal evaporation model', or 'NIE' model. Their model also predicts the shape of the $H_2{}^{18}O$ and $H^{2}HO$ (or HDO) profiles under non-isothermal conditions. With some modifications to the Barnes and Allison (1984) theory, a formulation can be derived to relate downward vapor flux to total recharge.

Prior to developing a model, some basic assumptions must

be made to characterize the system to be modeled. First, the movement of water is occurring in both the liquid and vapor phases in response to both thermal and moisture gradients. Formulations describing heat and moisture flow have previously been presented by Philip and de Vries (1957) and Taylor and Carey (1964). The main problem in applying these two theories is in estimating the various diffusivities. This is not as difficult however, if one is modeling the relative fluxes of the isotopic species in the water molecule, rather than the bulk fluid movement. The diffusivities of the isotope species vary little with changes in moisture content, unlike the liquid moisture diffusivity which can vary over orders of magnitude. The system under consideration is described as follows: quasi-steady, one-dimensional vertical flow of water vapor from a plane of zero flux at the evaporation front downward to the water table, and a downward advective liquid flux. These conditions occur at the Sevilleta site during the summer months when the vapor flux is probably greatest.

The various fluxes need to be separated into liquid- and vapor-phase components. Within the liquid phase, an advective-diffusive process is assumed. However, in the vapor phase there is only a diffusive component, which can be modeled according to Fick's law.

Other factors related to the behavior of the isotopes must also be addressed. Isotopic fractionation occurs when

the water changes state between a liquid and vapor phase. This is due to differences in chemical potentials between the isotopic species. The heavier isotopes tend to fractionate into the liquid phase relative to the lighter vapor phase. The result is a concentration gradient in the isotopic species. Differences in the isotopic diffusivities will also enhance the concentration gradient. Temperature effects on the model parameters can be accounted for by making these parameters functions of temperature.

Development of a model to describe the isotope profile and quantify the vapor flux is based on the works of Philip and de Vries (1957) and Barnes and Allison (1984). Assuming one-dimensional vertical flow, the equation for the liquid flux is given by Darcy's law, where:

$$q^l/\rho = -Ki = -Kd\Phi/dz = -Kd(-z+\psi)/dz \qquad (1)$$

The symbols are defined in Table 1. For the minor isotopes of hydrogen and oxygen in water, given a symbol i, there is both an advective and diffusive flux, such that:

$$q_i^l = q^l R_i - \rho D_i^* dR_i/dz \qquad (2)$$

The effective diffusivity of species i in the liquid water is determined by:

$$D_i^* = \gamma_i D_i \qquad (3)$$

where D_i is the molecular diffusion coefficient of species i in liquid water. The pore geometry factor, γ_i, accounts for the effect of tortuosity and changing water content. Barnes and Allison (1984) discuss the determination of

TABLE 1 - LIST OF SYMBOLS

Symbol	Description
D^*, D	(effective=*) self-diffusion coefficient of water [m^2/s]
D_i^*, D_i	(effective=*) diffusion coefficient of isotopic species i in liquid phase [m^2/s]
D^{v*}, D^v	(effective=*) diffusivity of water vapor in air [m^2/s]
D_i^{v*}, D_i^v	(effective=*) vapor diffusivity of isotopic species i in air [m^2/s]
h	relative humidity
i	subscript to denote isotopic species, either ^{18}O or ^{2}H
K	unsaturated hydraulic conductivity [m/s]
l	sub- or super-script to denote liquid phase
N^{sat}	saturated water vapor density in air [kg/m^3]
p	porosity
q^l, q^v, q_i^v, q_i^l	mass flux of water or isotopes [kg/m^2s]
$R_i^v, R_i, R_i^{res}, R_i^*$	isotope ratio
v	sub- or super-script to denote vapor phase
W	recharge rate [m/s]
z	depth below land surface [m]
z_l, z_v	characteristic length [m]
α_i^*	equilibrium fractionation factor
$\gamma^v, \gamma_i^v, \gamma_i, \gamma$	pore geometry factor
δ_i, δ_i^{res}	delta value
ϵ_i^*	equilibrium enrichment
η_i	diffusion ratio excess
θ	volumetric water content
ν, ν_i	mass flow factor
ρ	density of liquid water [kg/m^3]
σ_i, σ_i^v	diffusion ratio factor
Φ	total potential [m]
ψ	hydraulic or pressure head [m]

γ_i.

For the water vapor movement, Fick's law of diffusion is applicable, where:

$$q^v = -D^{v*}d(hN^{sat})/dz \quad (4)$$

Refer to Table 1 for parameter definitions. Both the effective diffusivity of water vapor, D^{v*}, and the saturated vapor density, N^{sat}, are dependent on temperature. Under non-isothermal conditions (i.e., where temperature changes with depth) these parameters will change with depth. The effective diffusivity of water vapor is defined as follows:

$$D^{v*} = \gamma^v(\theta)\nu D^v \quad (5)$$

A discussion on the determination of the mass flow factor, ν, and the pore geometry factor, γ^v, is given in Barnes and Allison (1984). The molecular diffusivity of water vapor in air, D^v, as a function of temperature, is given by Jaynes and Rogowski (1983).

For the minor isotopes of hydrogen and oxygen in water, the following vapor flux equation holds:

$$q_i^v = -D_i^{v*}d(R_i^v hN^{sat})/dz \quad (6)$$

Equation 5 can be adjusted for the isotope species to determine D_i^v.

The following equation relates the liquid to vapor isotope ratio:

$$R_i^v = \alpha_i^* R_i \quad (7)$$

The diffusivity of water vapor in air is related to the isotopic vapor diffusivity as:

$$\sigma_i^v = D^{v*}/D_i^{v*} = \gamma^v D^v/\gamma_i^v D_i^v \quad (8)$$

The equilibrium fractionation factor can be expressed as follows:

$$1 - \epsilon_i^* = \alpha_i^* \quad (9)$$

The diffusion ratio excess is presented as:

$$1 + \eta_i = \sigma_i \quad (10)$$

A vapor-length factor is given by:

$$z_v = N^{sat} D^{v*}/W\rho \quad (11)$$

The corresponding liquid-length factor is given as:

$$z_l = D^*/W \quad (12)$$

The isotope ratio is related to a standard, SMOW, and expressed as:

$$1 + \delta_i = R_i/R_i^*$$

Again, consult Table 1 for definitions of these parameters. The recharge rate, W, is equivalent to the deep flux of water below the root zone which eventually recharges the underlying ground water. The total recharge flux, q, can be represented as:

$$q = -W\rho = q^l + q^v \quad (14)$$

and

$$q_i = -W\rho R_i^{res} = q_i^l + q_i^v \quad (15)$$

Using the relationship defined by equation 11, equation 4 can be rewritten as:

$$q^v/(W\rho) = -hz_v d[\ln(hN^{sat})]/dz \quad (16)$$

from equation 6, and the expressions in equations 7, 8, and 11:

$$q_i^v/(W\rho) = -hz_v R_i \alpha_i^*/\sigma_i^v d[\ln(\alpha_i^* R_i h N^{sat})/dz \quad (17)$$

from equation 2, and the relations in equations 8 and 12 we obtain:

$$q_i^l/(W\rho) = q^l R_i/(W\rho) - z_l R_i/\sigma_i d[\ln(R_i)]/dz \quad (18)$$

Combining equations 14 through 18 to eliminate the flux terms and obtain an expression describing the profile shape yields:

$$hz_v R_i\{(1-\alpha_i^*/\sigma_i^v)d[\ln(hN^{sat})]/dz - (\alpha_i^*/\sigma_i^v)d[\ln(\alpha_i^* R_i)]\} = R_i - R_i^{res} + (z_l/\sigma_i)dR_i/dz \quad (19)$$

Making additional substitutions from parameters defined above, dropping terms of second order, assuming η_i does not vary with depth, h is close to unity, and rearranging:

$$d\delta_i/dz + [(\delta_i-\delta_i^{res})/(z_l + z_v)] = z_v[(\epsilon_i^* + \eta_i)/(z_l + z_v)]d[\ln(N^{sat}(\epsilon_i^* + \eta_i))] \quad (20)$$

Equation 20 is useful in determining the shape of the profile for a given isotopic species of hydrogen or oxygen in water, preferably deuterium. This equation can be solved numerically, taking into account the temperature dependence of the various parameters.

Equations 14 through 18 may also be combined to obtain the ratio of the total vapor flux to the total recharge flux. The following expression is the result:

$$-q^v/(W\rho) = (\epsilon_i^* + \eta_i)^{-1}[\delta_i - \delta_i^{res} + (z_v + z_l)d\delta_i/dz - z_v d\epsilon_i^*/dz] \quad (21)$$

The last term in equation 21 is the non-isothermal component

to the vapor flux.

If the recharge flux is estimated by an independent method, then the quantification of the vapor flux can be made quite readily. In this study the recharge flux can be estimated through the use of the bomb-pulse tritium as a tracer. The rate of tritium movement has been quantified by Phillips et al. (1988).

A numerical model has been written to solve equations 20 and 21. In solving equation 20, a non-linear least-squares optimization approach has been used to fit the model to an observed set of data. A Marquardt solution was used for the least-squares approach. Certain parameters may be specified as fitted variables: vapor tortuosity factor, liquid tortuosity factor, δ_1^{res}, recharge rate (W), and the slope and intercept of an exponential temperature versus depth relation. Limits may be placed on the bounds of each fitted variable, or the variables may be held constant at the users' discretion. This numerical approach is henceforth referred to as the 'non-isothermal recharge' model, or 'NIR' model.

Allison et al. (1984) presented an independent technique for calculating the recharge flux from stable-isotope-profile data. The system under consideration is one in which piston displacement and mixing are the primary mechanisms causing the recharge flux. Their technique will henceforth be referred to as the 'piston displacement/mixing' model, or 'PD/M' model. The PD/M model assumes that a series of

precipitation events, all with the same isotopic composition, infiltrate episodically into the soil. Between rainfall events the soil water has a chance to evaporate, and hence become more enriched isotopically. The next precipitation occurrence displaces this heavier water downward in the profile, and the waters mix. If this cycle happens with some degree of regularity, the composition of the soil water on average should be displaced relative to the meteoric water line, but still maintain the meteoric water line slope. Therefore, a plot of ^{2}H versus ^{18}O should contain a linear array of data that is some distance to the right of the meteoric water line. The difference in deuterium excess values for this data versus the meteoric water line can then be used to estimate recharge.

Allison et al.(1984) have plotted the displacement of δD from the meteoric water line against the inverse of the square root of recharge. Their recharge estimates for calibrating this model are from tritium and chloride mass balance techniques. The lower the recharge rate, according to this model, the greater the relative deuterium displacement. Conversely, the higher the recharge rate the closer the isotope values will lie to the meteoric water line. For recharge rates greater than 1 cm/yr, the deuterium displacement becomes so small that the technique loses its sensitivity.

RESULTS

In order to use the theory presented in the previous section, a number of soil profiles were obtained throughout the term of the project. The seven profiles sampled cannot all be used in evaluating the vapor flux contribution to recharge, inasmuch as some of the earlier data were needed to refine preparation and analytical techniques. Data obtained in the sampling of these profiles, both isotopic and soil moisture related, are presented in Appendix A. All profiles were collected at the Sevilleta National Wildlife Refuge research site. More specifically, the cores were taken at the same locale that Phillips et al. (1988) sampled for bomb-pulse ^{36}Cl and ^{3}H, and adjacent to the site investigated by Stephens and Knowlton (1986).

The first core was taken during the fall of 1986. The Sevilleta Stable Isotope Profile 1, SSIP1, was sampled from land surface to a depth of 5.0 meters with the NMEID auger rig. The soil water was distilled from each subsample with the azeotropic toluene distillation technique, described above. The CO_2/H_2O equilibration technique was used to obtain CO_2 gas to analyze at Yale University. These samples contained enough toluene contamination so as to interfere with the mass spectrometric analyses. Owing to the relatively small water volumes obtained from these subsamples,

additional isotopic work could not be performed on this core.

The second core from the site, SSIP2, was also obtained with the aid of the EID drill rig. This core was drilled to a depth of 5.0 meters in September 1987. Again, azeotropic toluene distillations were performed to extract the soil water from the subsamples. Special precautions were taken in purifying the soil water of dissolved toluene. This involved the repeated application of a paraffin absorbent. Oxygen analyses were performed at the University of New Mexico. Despite the added precautions, these samples also proved to be contaminated with toluene. The azeotropic toluene distillation procedure was then considered inadequate for consistent reproducibility. At this point a new vacuum distillation procedure was developed and tested, as discussed above.

The third core, SSIP3, was hand augered on April 20, 1988 to a depth of 4.40 meters. The new vacuum distillation technique was used to obtain the soil-water samples. The oxygen-18 data were analyzed at two different laboratories, the University of Missouri laboratory at St. Louis, MO, and the U.S. Geological Survey (USGS) laboratory in Reston, VA. The depth versus $^{18}O/^{16}O$ ratio for this core is shown in Figure 6. The hydrogen was obtained from these samples using the zinc reduction technique, discussed above. The $^{2}H/H$ ratios were obtained at the University of New Mexico. Figure 7 shows the depth versus $^{2}H/H$ ratios for SSIP3. Appendix A

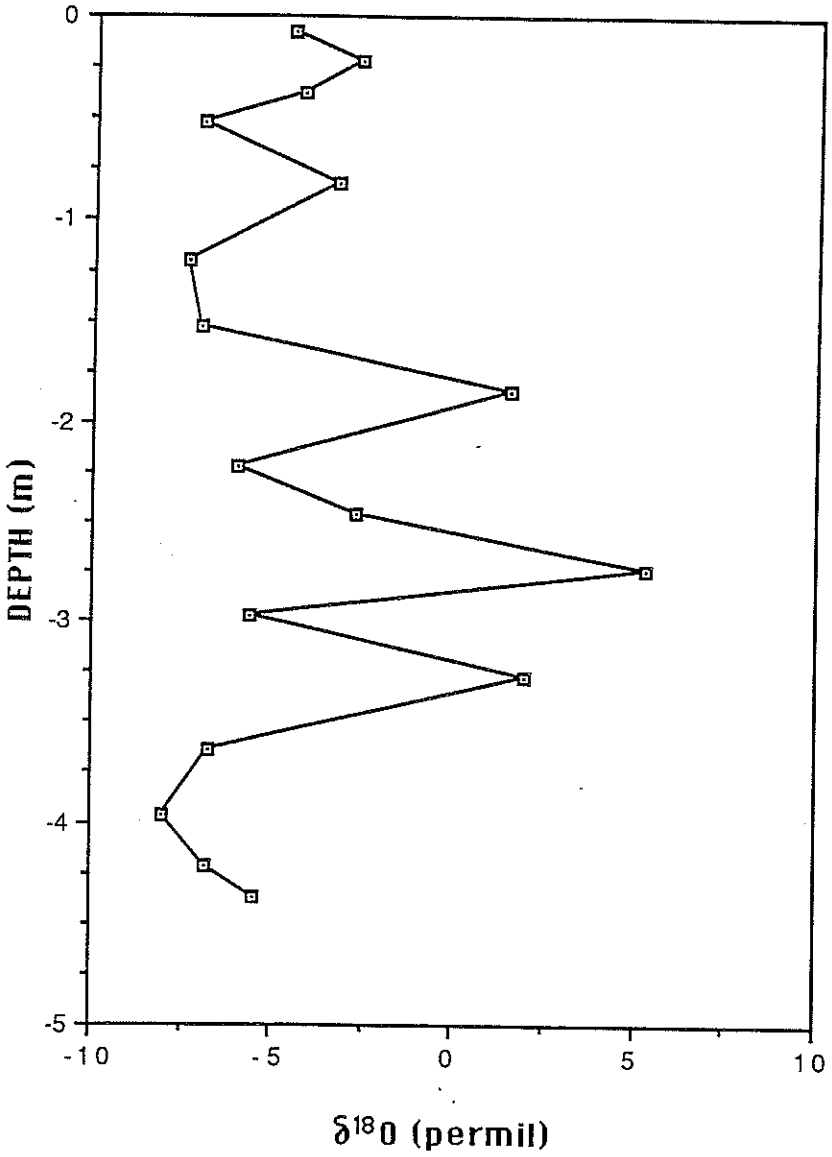

Figure 6. Depth versus $\delta^{18}O$ for SSIP3 core

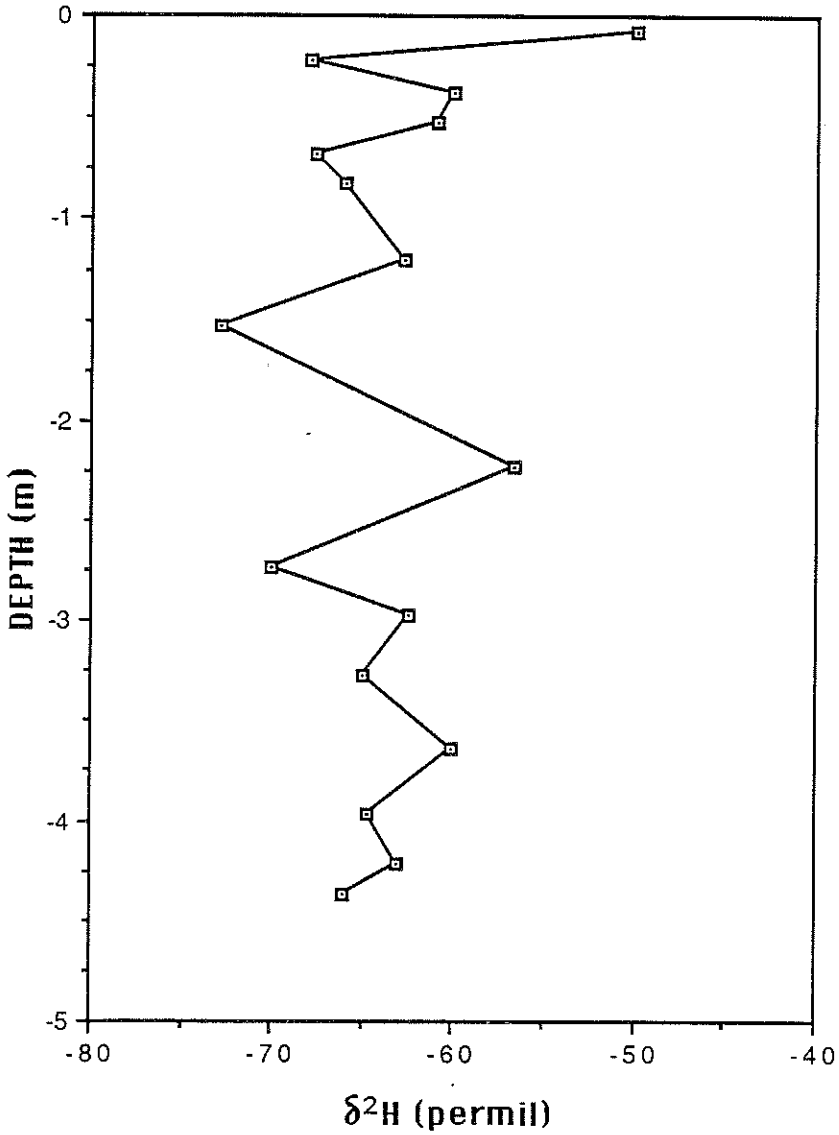

Figure 7. Depth versus δ^2H for SSIP3 core

contains the isotopic, water content, and temperature data versus depth for this core.

Data from SSIP3 were not of sufficiently high quality to use for the determination of recharge, for several reasons. First, considerable scatter in the isotope ratios with depth is apparent from Figures 6 and 7. This scatter is probably due to the inadequacies of the distillation technique at the time. Refinements in the distillation procedure were made to correct for this problem, as discussed in the distillation section above.

In addition, the data obtained from the University of Missouri were potentially in error due to a machine malfunction. Unfortunately, the mass spectrometer at Missouri had developed a leak in the inlet system, causing fractionation of the standard gas, and consequently erroneous results. Correction factors were formulated and applied to the ratio data. These data, in conjunction with the data obtained from the USGS lab, make a very irregular plot of depth versus oxygen-18. Also, several duplicate samples were sent to both labs, with markedly different results. The Missouri data are considered most suspect, owing to the machine breakdown. However, the number of oxygen-18 data from the USGS analyses is insufficient to adequately define the profile.

The hydrogen data from SSIP3 also exhibit considerable scatter with depth, even though all isotopic analyses were

performed at UNM. Again, this is probably due to developmental problems with the distillation procedure at the time. In addition, the profile does not have an adequate depth discretization within the top 30 cm or so to define the characteristic shape of the profile. Therefore, this core was considered a test case for defining better sampling and preparation techniques for the next profile.

The fourth soil profile collected, SSIP4, was sampled to a depth of 5.0 meters by hand augering on May 17, 1988. This profile was sampled a few days after a precipitation event (Stein, T., personal communication, May 17, 1988). Figure 8 shows the precipitation versus time at the Sevilleta site over several months of this year. Refinements in the vacuum distillation technique were applied during preparation of these samples. The oxygen-18 and deuterium analyses were performed at the New Mexico Institute of Mining and Technology. Figures 9 and 10 show the depth versus ^{18}O and depth versus ^{2}H, respectively, for SSIP4.

The data presented in Figures 9 and 10 show some scatter, in comparison to the relatively smooth profiles reported previously in the literature (e.g. Allison et al. 1984). Sources of error probably include insufficient distillation times and/or improper sealing of the soil-water storage bottles. These problems have been addressed in the methods section above.

On August 4, 1988, two soil cores were obtained at the

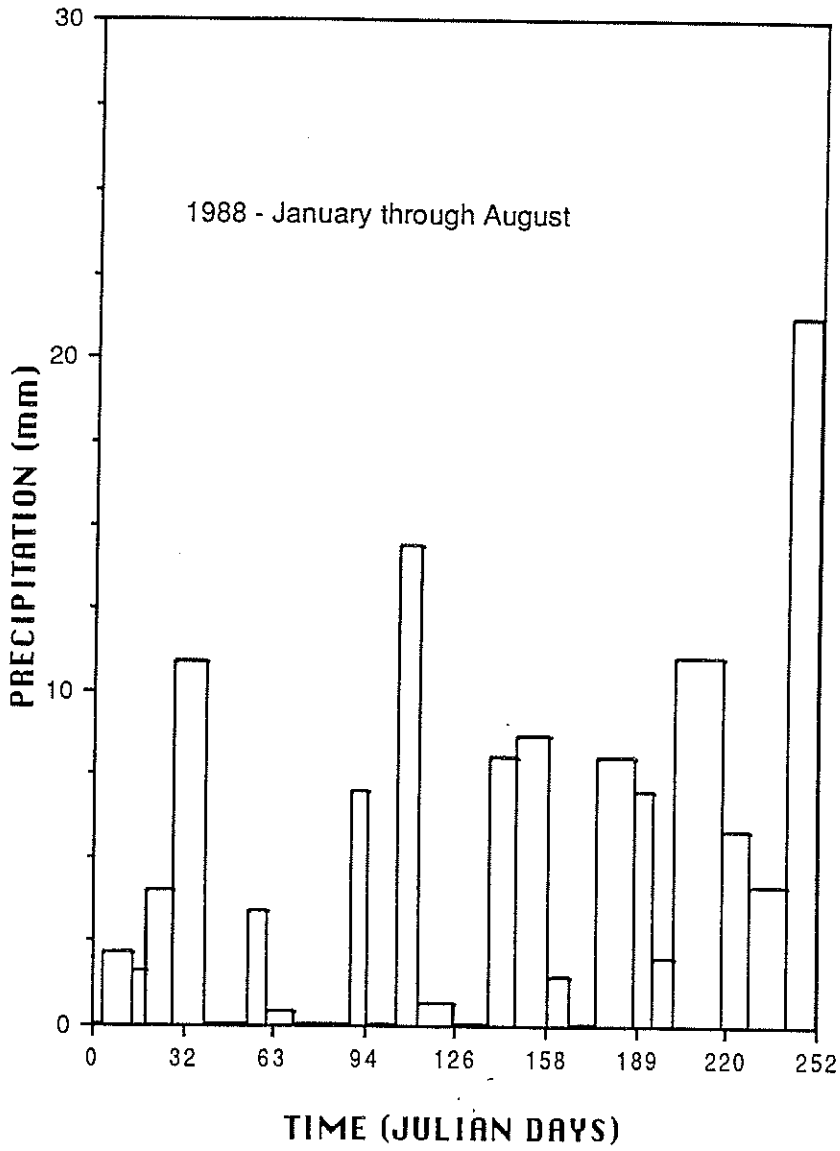

Figure 8. Time versus precipitation

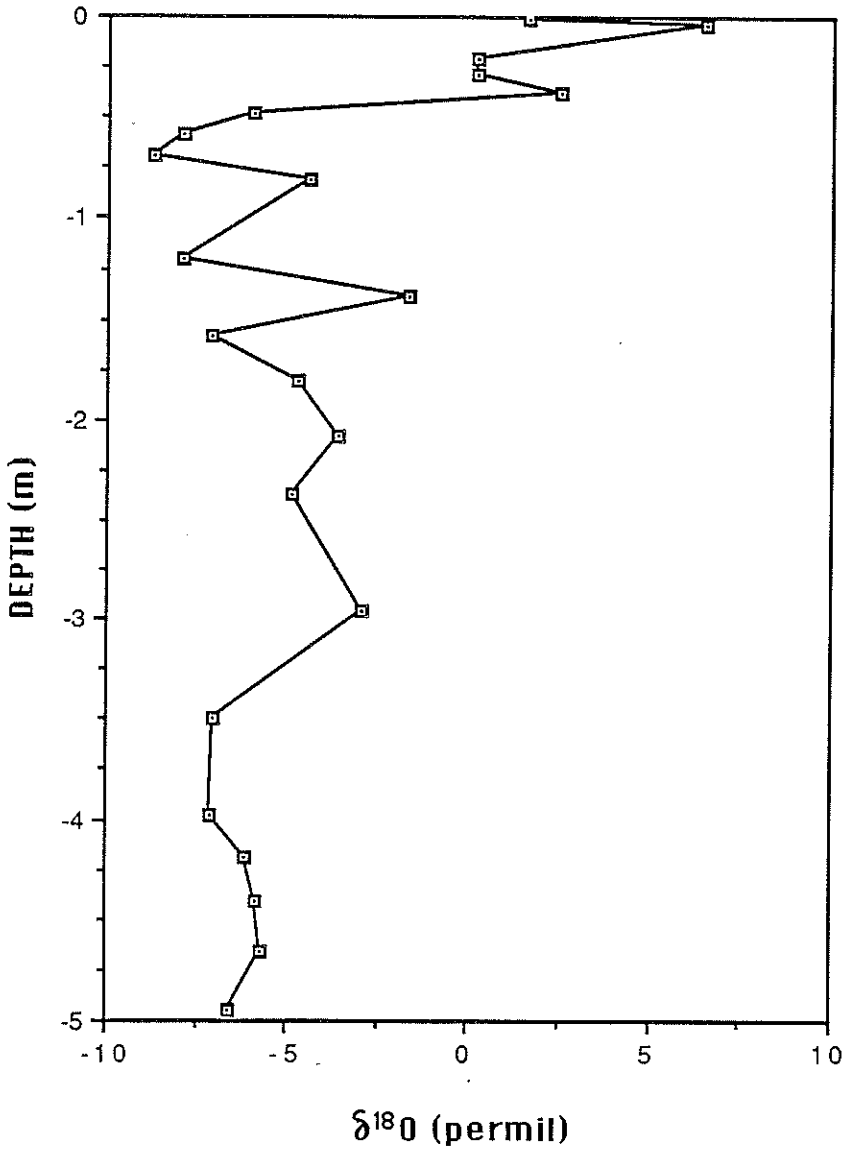

Figure 9. Depth versus $\delta^{18}O$ for SSIP4 core

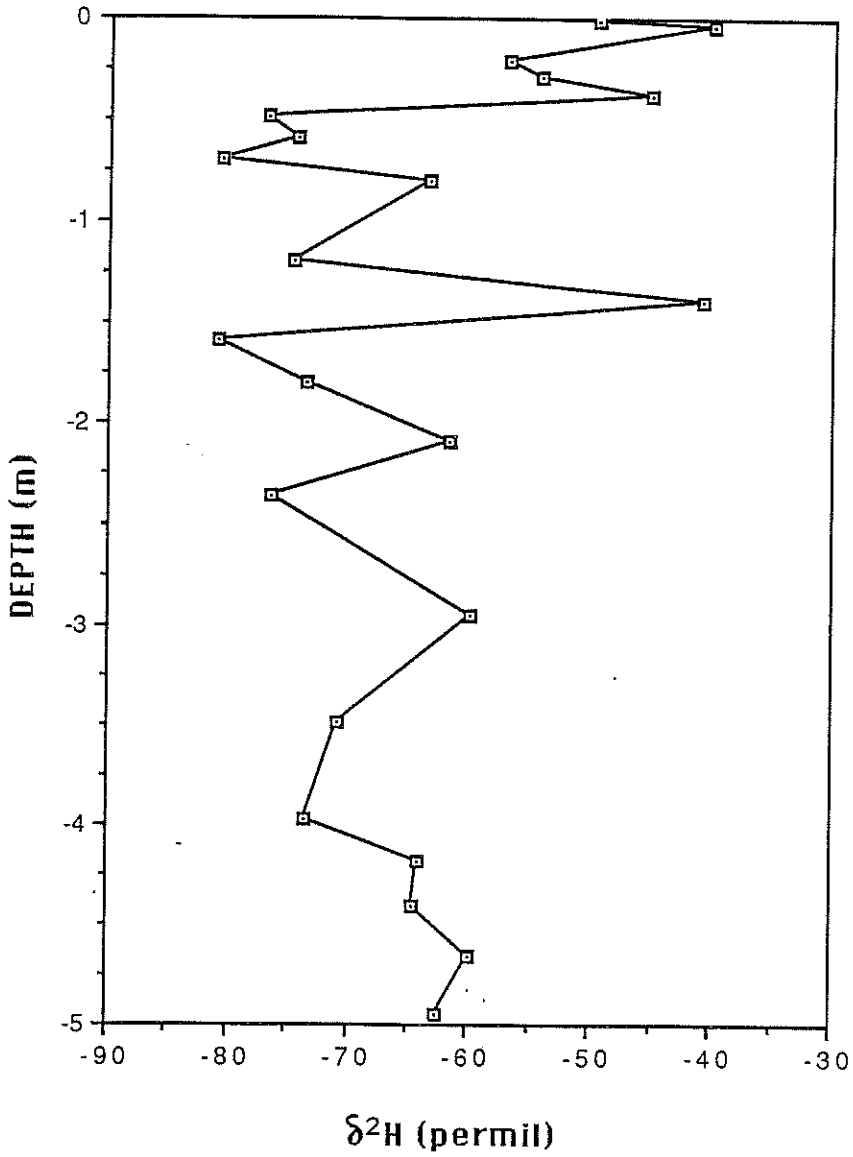

Figure 10. Depth versus δ^2H for SSIP4 core

Sevilleta research site, SSIP5 and SSIP6. The two borings were made approximately 70 cm apart. The reason for obtaining duplicate cores was to assure reproducibility in the sampling and processing of soil cores. The concern over reproducibility stems from the variability observed in the SSIP4 profile. The SSIP5 and SSIP6 cores were hand-augered to depths of 4.55 and 3.40 meters, respectively.

The vertical discretization of sampling within the SSIP5 core was increased, relative to the other profiles collected at the site, to define better the characteristic shape of the isotope profiles. Figures 11 and 12 show the depth versus ^{18}O and depth versus ^{2}H profiles, respectively, for the SSIP5 core. The variability within these profiles is relatively small. Figure 13 depicts both the ^{18}O and deuterium against depth, showing the relative differences in behavior for both isotopic species within the profile. Figure 14 is a plot of deuterium versus oxygen-18, with the corresponding meteoric water line (MWL) for this area (Vuataz and Goff 1986).

Data from the SSIP6 profile corroborate the SSIP5 profile. Figure 15 depicts the depth versus water content for both the SSIP5 and SSIP6 cores. There is considerable variability in moisture content between the two cores, despite their close proximity to each other. These differences in moisture are attributed to spatial variability. Figure 16 shows a plot of depth versus deuterium for both the

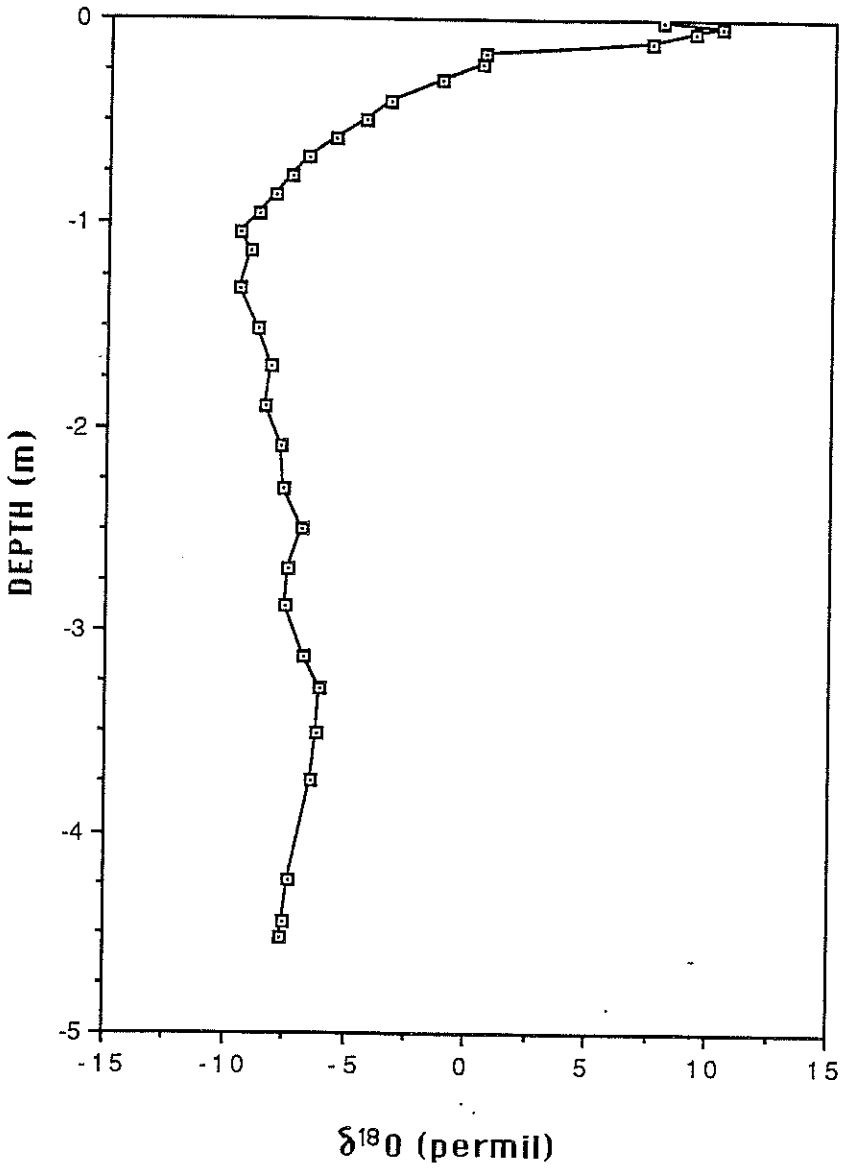

Figure 11. Depth versus $\delta^{18}O$ for SSIP5 core

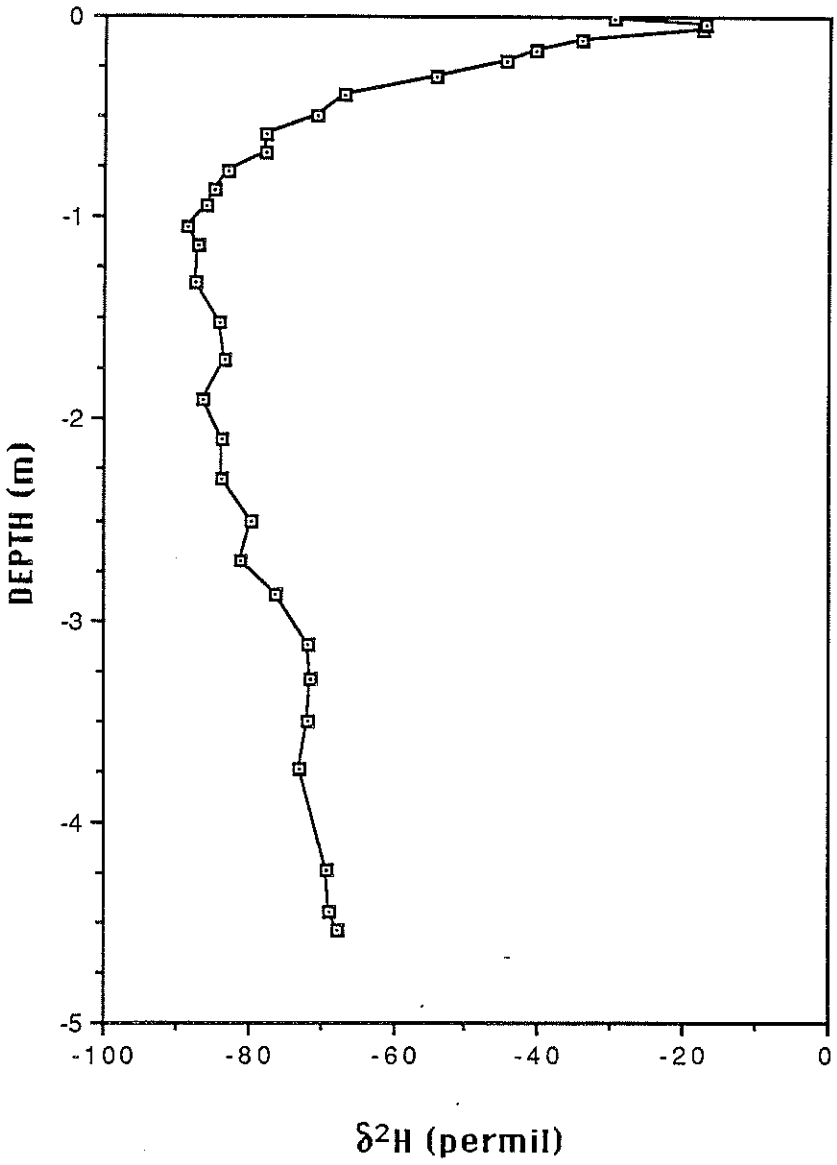

Figure 12. Depth versus δ^2H for SSIP5 core

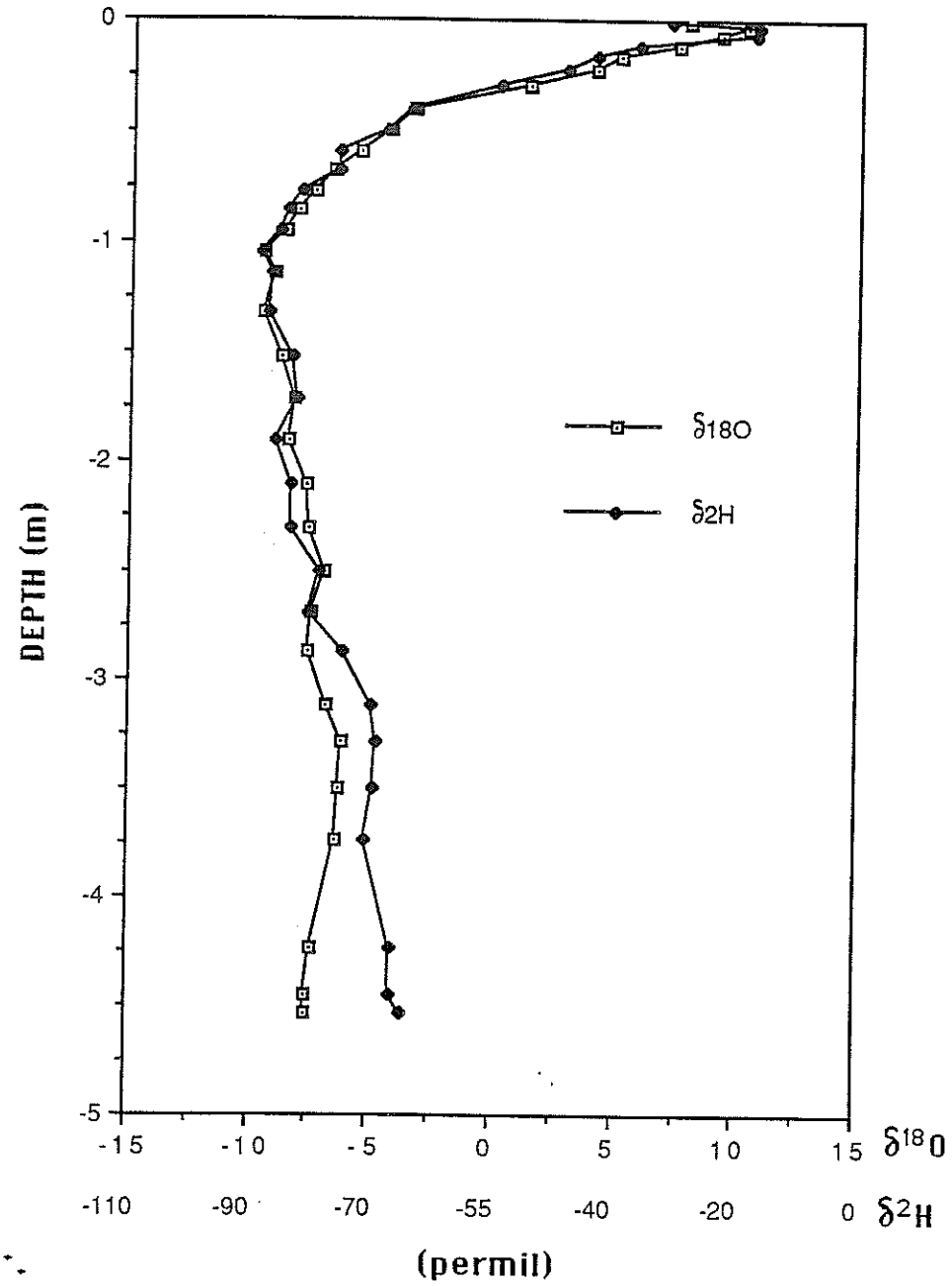

Figure 13. Depth versus δ^2H and $\delta^{18}O$ for SSIP5 core

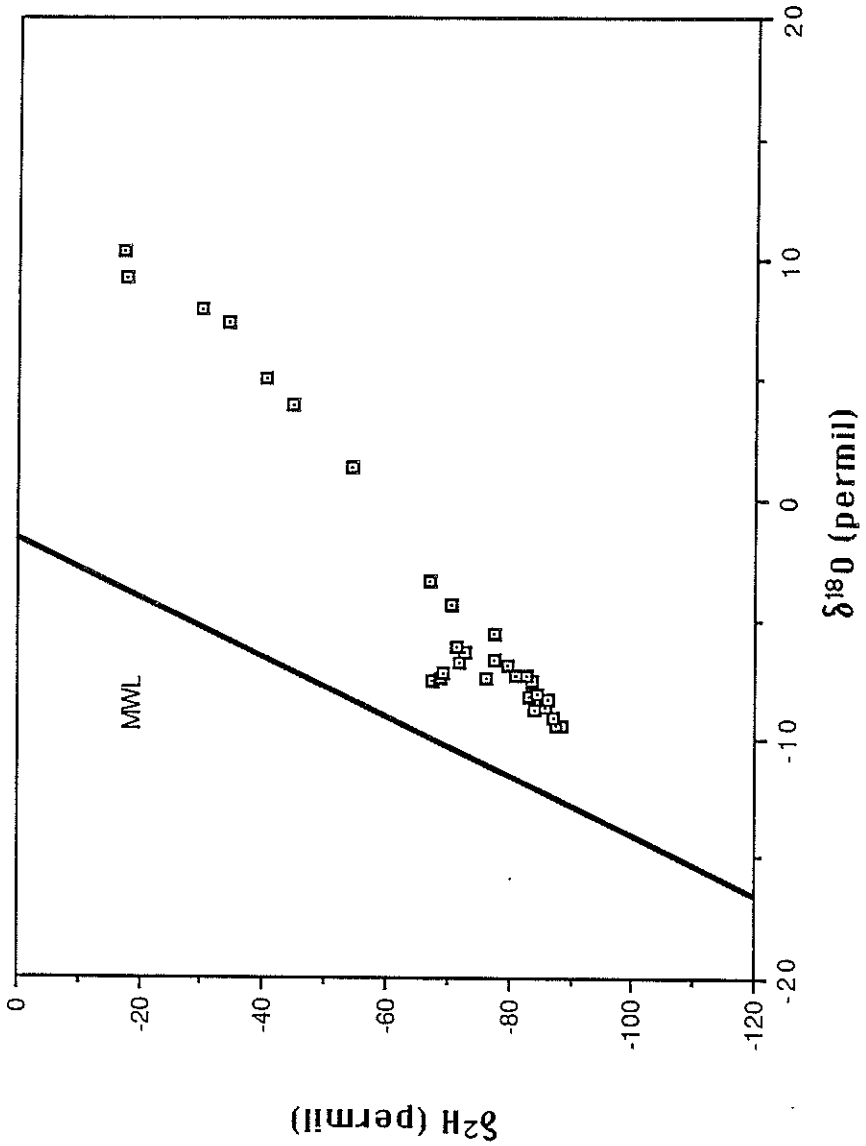

Figure 14. δ^2H versus $\delta^{18}O$ for SSIP5 core

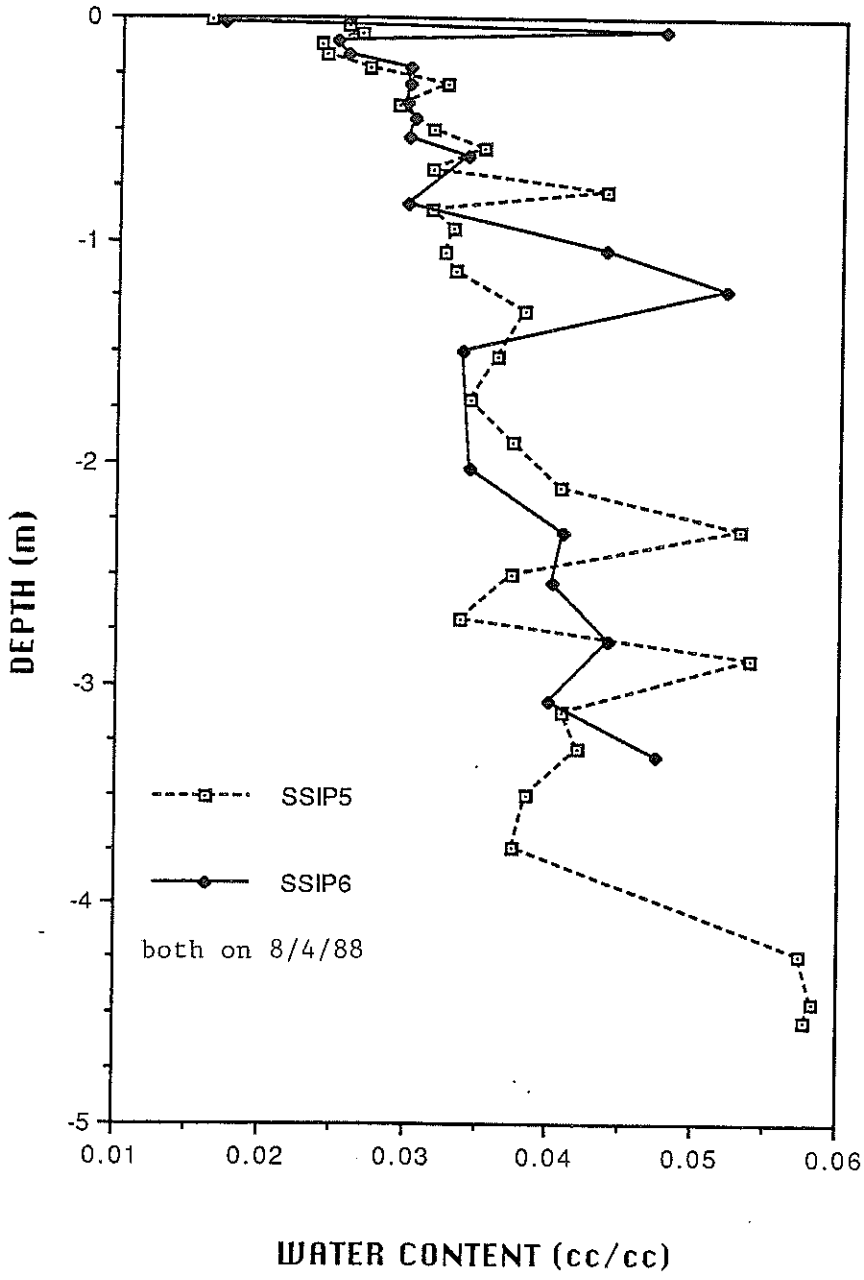

Figure 15. Depth versus water content for SSIP5 and SSIP6 cores

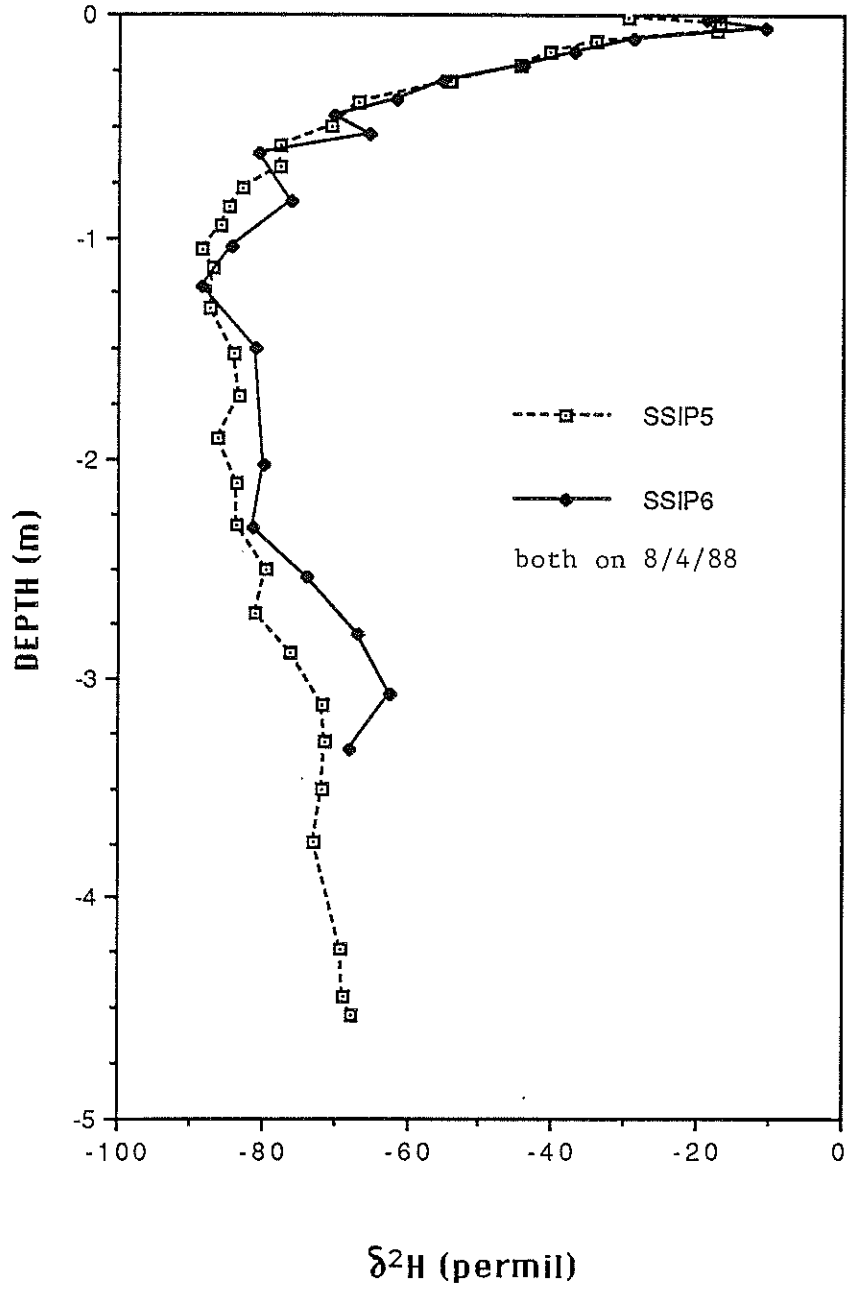

Figure 16. Depth versus δ^2H for SSIP5 and SSIP6 cores

SSIP5 and SSIP6 cores. The two profiles are markedly similar, despite the observed variability in water content. All the data obtained from these cores are presented in Appendix A.

On October 27, 1988 a seventh core, SSIP7, was taken at the Sevilleta site. During the 'rainy season', August through October, 1988, there was an appreciable amount of precipitation occurring at the site. Figure 17 shows a plot of depth versus water content for both the SSIP5 and SSIP7 cores. The SSIP7 profile exhibits a pronounced elevation in moisture content above a 1 meter depth, relative to the SSIP5 profile. This increase in moisture is indicative of an infiltration and mixing process occurring between August 4 and October 27. Figure 18 is a plot of depth versus deuterium for the SSIP5 and SSIP7. The differences in isotopic composition between the two profiles in the upper meter is also supportive of an infiltration and mixing process, the implications of which will be discussed below.

Application of the numerical techniques outlined in the previous section on numerical modeling methods will yield an estimate of the vapor flux contribution of the soil-water movement that leads to recharge. The NIR model is limited to quasi-steady state conditions. Of the seven cores collected, only the SSIP5 and SSIP6 profiles satisfy this criteria. Of these two profiles, both of which were collected on the same day, the SSIP5 core was discretized into finer sampling

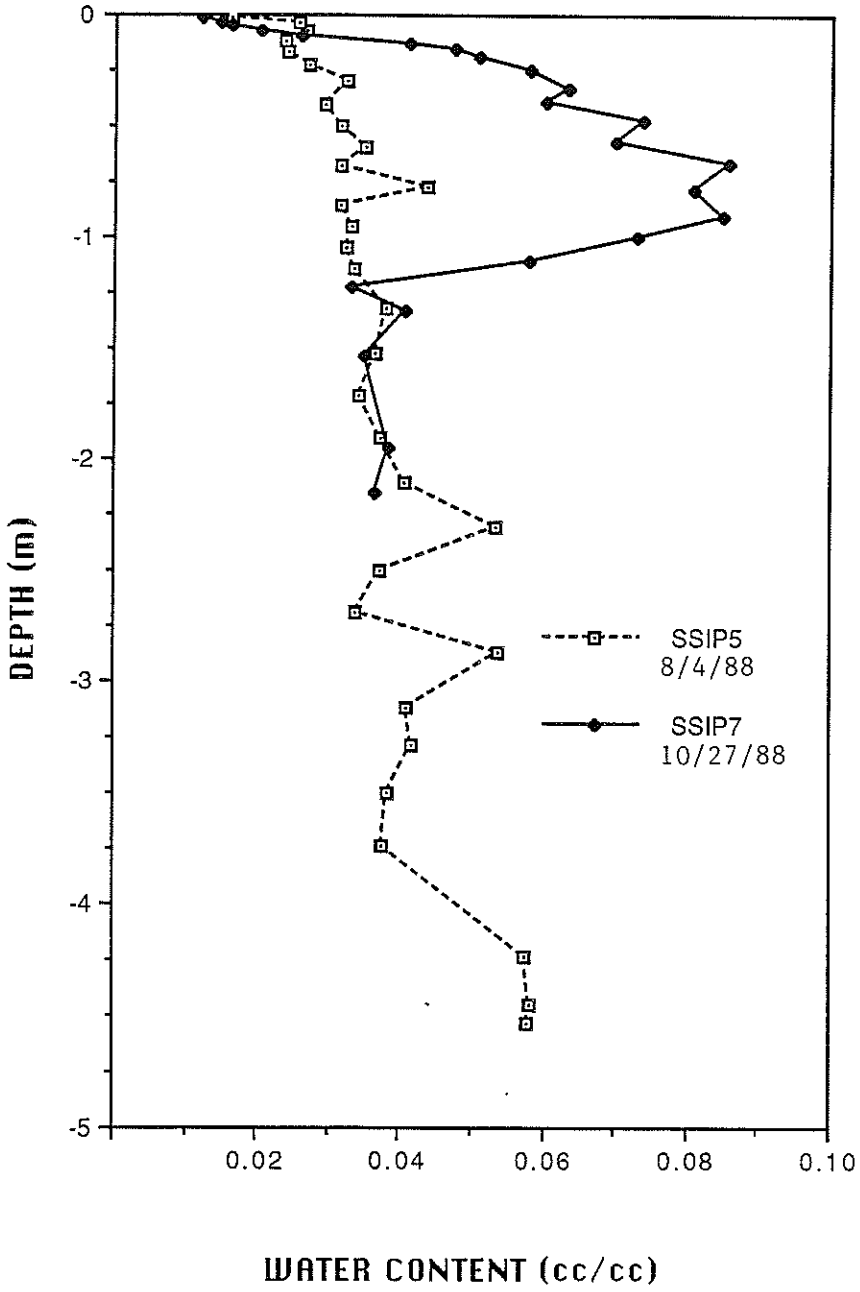

Figure 17. Depth versus water content for SSIP5 and SSIP7 cores

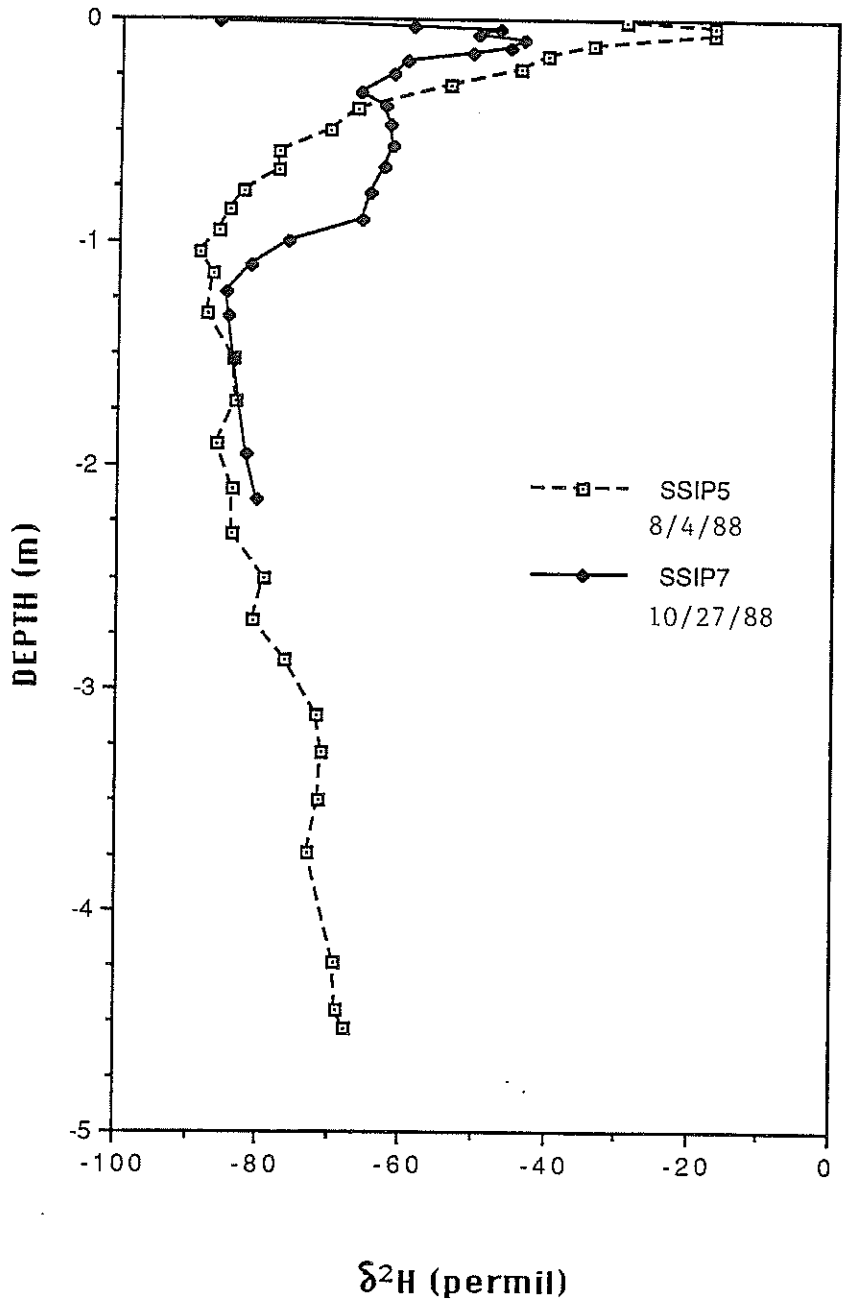

Figure 18. Depth versus δ^2H for SSIP5 and SSIP7 cores

intervals and consequently has more data associated with it. The SSIP5 core is therefore preferred for analysis over the SSIP6 core. The SSIP7 core was collected at a time when the soil-water movement is presumed to be under transient conditions, during which redistribution is taking place. Therefore, SSIP7 is not suitable for analysis with the NIR model. The first step in the NIR modeling procedure is a determination of input parameters to equation 20. Equation 20 describes the shape of the isotope profile. Figure 12 shows the results of sampling for depth versus deuterium for the SSIP5 core. Deuterium is preferred over oxygen-18 for this analysis (Barnes and Allison 1984). Their conclusion was based on the fact that the kinetic fractionation is relatively insensitive to temperature, and ^{18}O is much less sensitive than deuterium. Therefore, the effect of temperature on the isotope profiles is relatively greater for deuterium than ^{18}O. Matching the observed deuterium data with the theoretical model should provide a qualitative estimate of the reliability of the input parameters to the model. For this analysis, the curve-matching technique was performed over the 0.12 to 2.70 meter depth interval. This zone corresponds to the liquid- and vapor-phase flow region below the evaporation front, but above the zone in which the water table influences the stable isotopic composition in the profile.

Many of the parameters required for the numerical

solution to equation 20 can be expressed as functional relationships with temperature or depth. Parameters such as ϵ_D^*, N^{sat}, D^v, and D^l are given in the literature as functions of temperature (from Majoube 1971; Weast 1975; Jaynes and Rogowski 1983; and Mills 1973; respectively). The water content versus depth relationship determined from field sampling may be regressed and expressed mathematically. This is also true of the temperature versus depth relation. The diffusion ratio excess, η_D, is taken from Merlivat (1979). The parameter estimations with the least degree of confidence are probably the mass flow factors and tortuosity terms. The recharge rate, W, is assumed to be equivalent to the specific flux determined from the bomb tritium over the past 20 years, 0.84 cm/yr (Phillips et al. 1988).

A non-linear least-squares optimization approach was taken to evaluate the goodness of fit between equation 20 and the observed deuterium data. The fitted variables in this analysis were δ_D^{res}, the liquid tortuosity factor, and the vapor tortuosity/mass flow factor. Two realizations of the temperature profile have been utilized to investigate the effect of temperature on the curve-fitting procedure and the vapor flux determinations. The depth versus temperature profiles for cases A and B are shown in Figures 19A and B. Case B has a larger temperature gradient in the upper portion of the profile than case A.

Figures 20A and B show the results of the curve-fit-

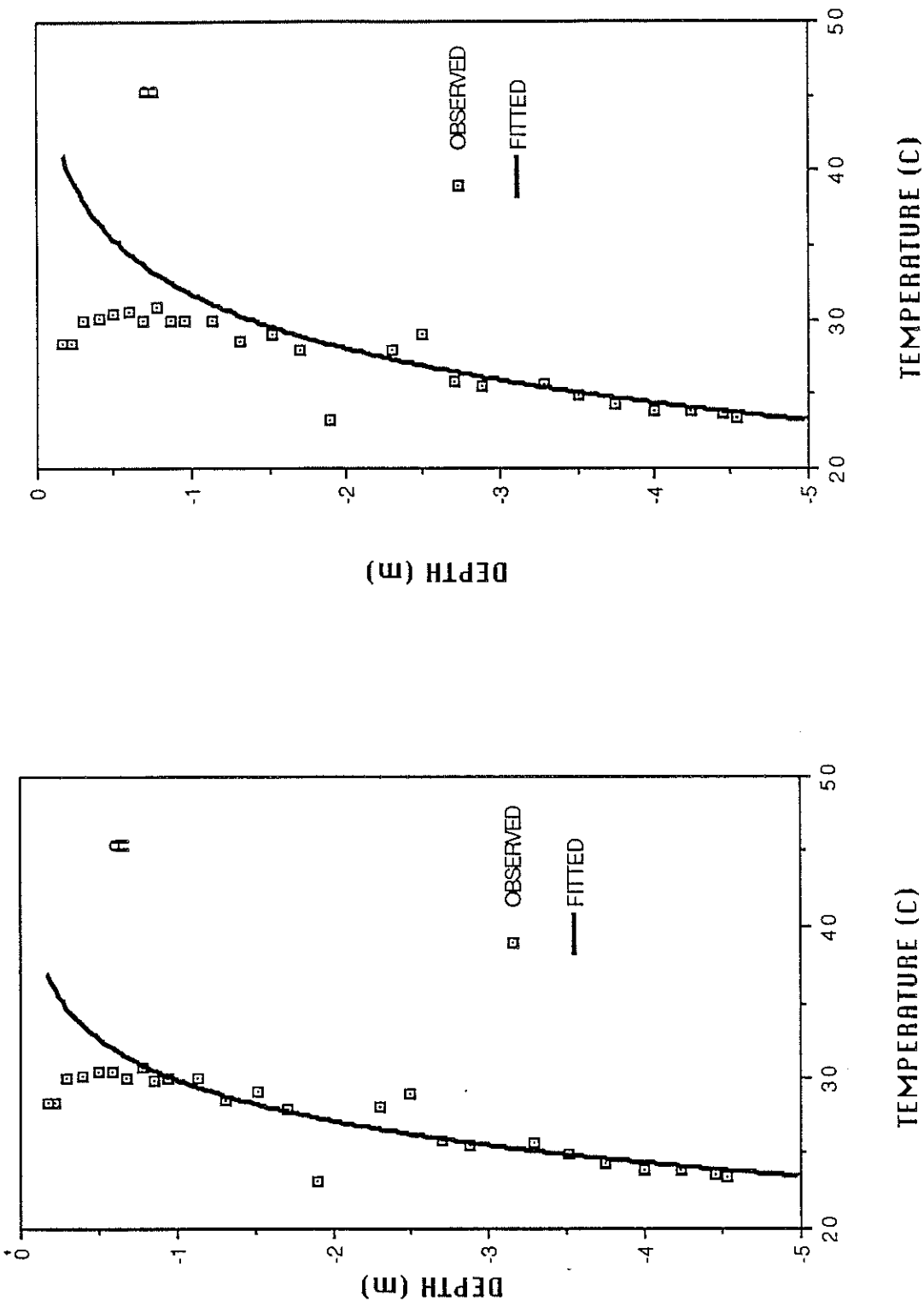

Figure 19. Depth versus temperature, for observed data collected at time of sampling, and for two temperature realizations for (A) case A data and (B) case B data

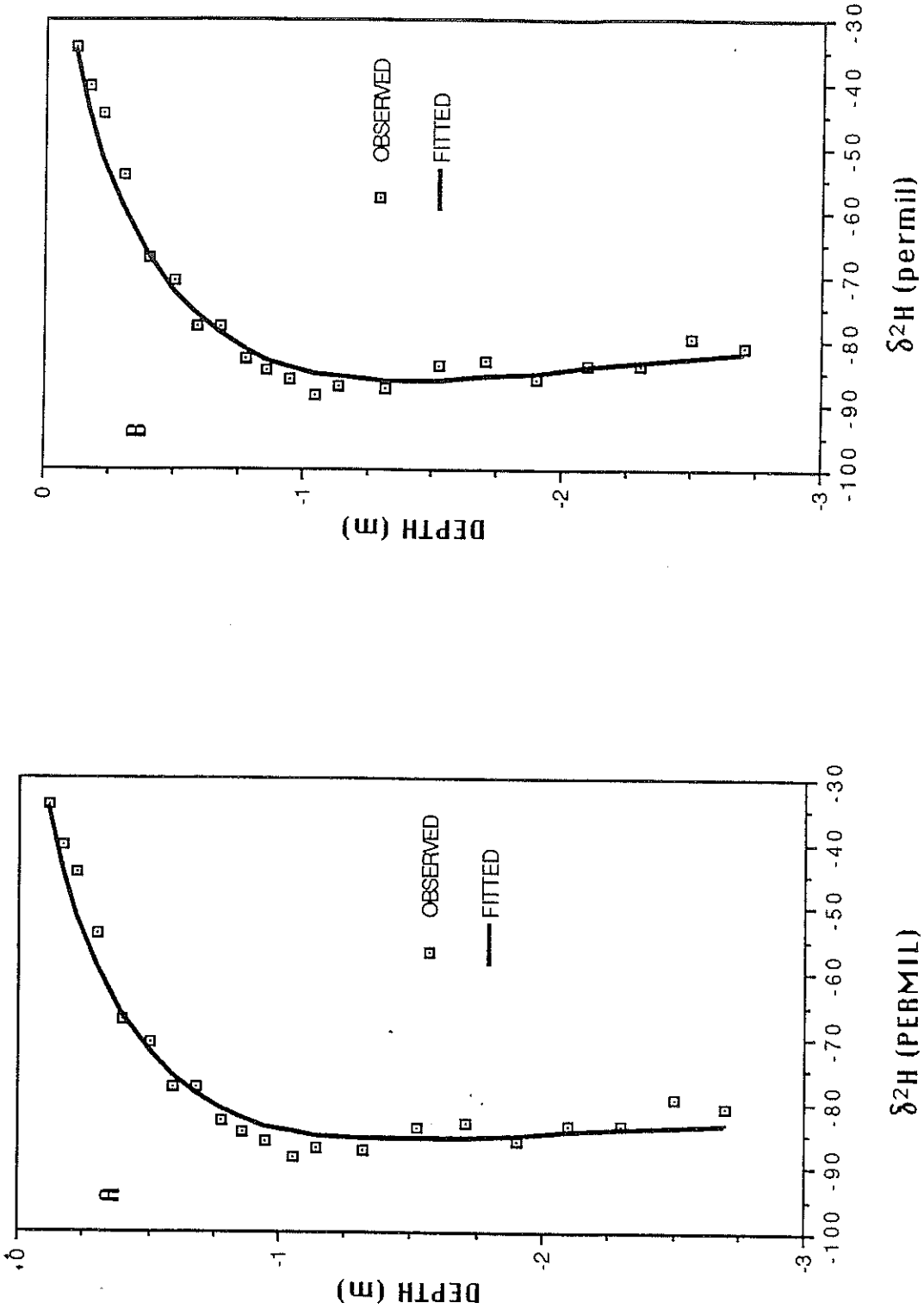

Figure 20. Depth versus fitted and observed δ^2H for SSIP5 core for (A) case A data and (B) case B data

ting, for the fitted versus observed deuterium profile. The curve-fitting statistics for the case B temperature realization yielded a slightly lower sum of the squares of the residuals than for case A. In other words, the case B data were a better fit to the observed data than case A data. The resultant values of δD^{res} were $-80.5^{o}/_{oo}$ (permil) for case A, and $-75.3^{o}/_{oo}$ for case B. The tortuosity factors for the effective vapor diffusivity were estimated at 0.423 and 0.611, respectively for case A and B. Barnes and Allison (1984) suggested a value of 0.667 for the vapor tortuosity factor. The effective tortuosity/mass flow factor for the liquid diffusivity was minimized at 0.03 in both cases, as calculated by Phillips et al. (1988) using previously published techniques. The implications of these differences will be discussed below.

Having achieved an adequate fit between the model and observed data in both cases, the next step was to estimate the relative contribution of the vapor flux to the recharge process. Equation 21 was solved numerically using the input and fitted parameters mentioned above for the same two cases. The liquid flux was computed using equation 14. The liquid and vapor fluxes are computed as fractions of the deep flux of soil water, or recharge. Figures 21 and 22 show the results of these analyses for cases A and B, respectively. In summary, the results indicate that between the 0.12 and 2.70 meter depths, the vapor flux component of

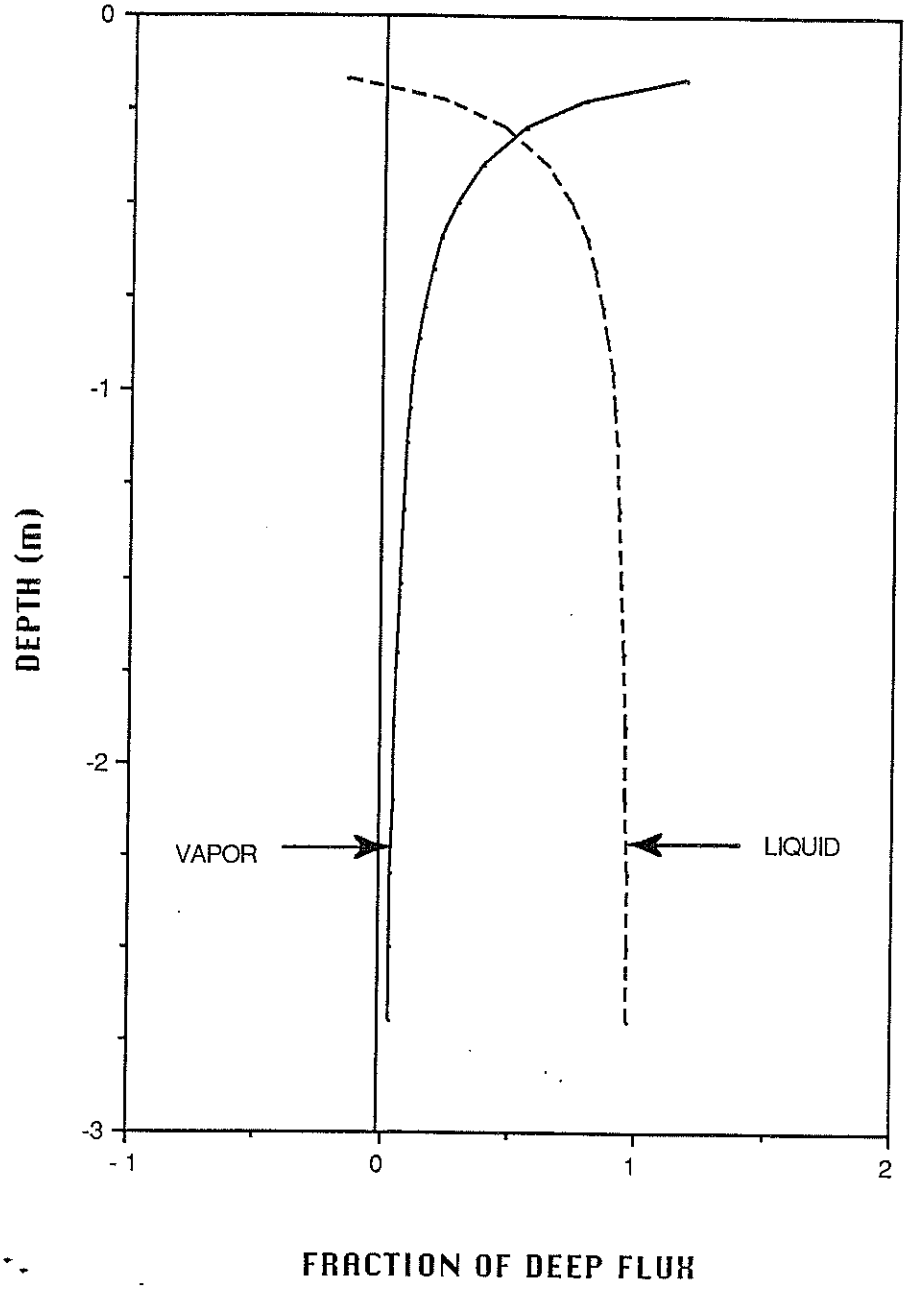

Figure 21. Depth versus fraction of deep flux, vapor and liquid flux to deep flux ratios for SSIP5 core, case A

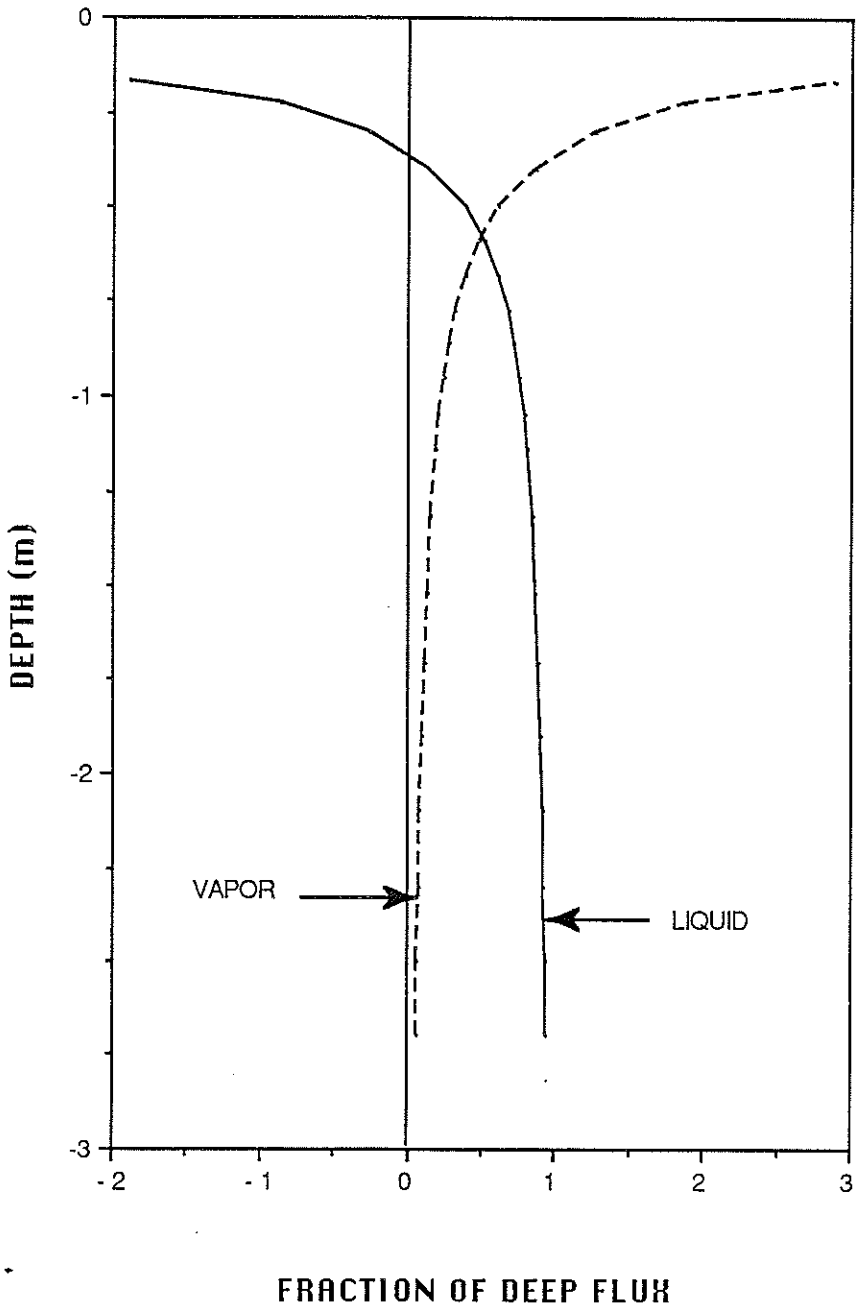

Figure 22. Depth versus fraction of deep flux, vapor and liquid flux to deep flux ratios for SSIP5 core, case B

soil-water movement, expressed as a vapor flux/deep flux ratio, exponentially decreases from 120 to 3% for case A, and 290 to 6% for case B. A depth-averaged approximation of this data yields values of 15 to 33 percent for the vapor/deep flux ratio. The negative values of the liquid/deep flux fraction are indicative of upward soil-moisture movement. As mentioned earlier, these results are for a profile sampled at only a single time, and not necessarily indicative of the long term average flux at the site.

The final technique discussed in the numerical modeling methods section above involves the calculation of the recharge flux by the PD/M model. Figure 14 shows the ^{2}H versus ^{18}O data from the SSIP5 core plotted with the meteoric water line. A line could be drawn through the lightest portion of this data, parallel to the meteoric water line (a slope of 8), to define the deuterium displacement. The deuterium displacement is estimated at $22^{o}/_{oo}$. The corresponding recharge flux, from the graph in Allison et al. (1984), is estimated at 0.083 cm/yr. This estimate is one order of magnitude smaller than the estimate of recharge based on the tritium transport.

DISCUSSION

The quantitative numerical analysis of the vapor flux presented above for the NIR model contains several assumptions worth discussing. First, the model assumes a one-dimensional vertical flow. The vapor flux is downward in response to temperature induced vapor pressure gradients. The liquid flux contains both an advective and diffusive component. The advective liquid flux (below the zone of evaporation) is assumed to be vertically downward. This condition is probably met during the summer months, when the vapor flux is greatest. Therefore, data from the SSIP5 core, sampled at the beginning of August 1988, can be used to model the vapor flux with these model criteria.

The tortuosity and mass flow factors determined in the modeling procedures are different from those reported in the literature. The tortuosity/mass flow factor for the effective liquid diffusivity was minimized at 0.03, as calculated by Phillips et al. (1988). For the effective vapor diffusivity there is a slight difference between fitted versus published tortuosity/mass flow factor values. The fitted model values for this term were 0.423 and 0.611 for cases A and B, respectively. Barnes and Allison (1984) have suggested a tortuosity/mass flow factor of 0.667. The differ-

ence in these estimates implies that the actual vapor flow has a slightly more tortuous path than can be accounted for by empirical estimation techniques.

The quantitative estimates of the vapor flux are consistent with the findings of Phillips et al. (1988). The vapor flux estimates within the 0.12 to 2.7 meter depth interval are 15 to 33 percent of the deep flux of soil-water movement, or recharge flux. In Figures 21 and 22, the point at which the liquid and vapor flux curves intersect is indicative of the separation between the vapor and liquid dominated transport zones. In other words, above this point of intersection the vapor-phase component of soil-moisture movement is dominant, and below it the liquid flux prevails. For cases A and B, the point of change for vapor versus liquid dominance is approximately 0.35 and 0.55 meters, respectively. As mentioned above, the zone in which the liquid flux curve in Figures 21 and 22 is negative constitutes upward flow. The point at which the liquid/deep flux ratio equals zero is indicative of a divergence of flow, a null point or point of zero flux. In other words, the liquid flux above this null point is upward, and below it the flow is downward. For cases A and B, the liquid flux null point is estimated at 0.20 and 0.35 meters depth, respectively.

The analyses just presented allow us to draw some conclusions with regard to the relative importance of the

vapor flux contribution to soil-water movement. During summer months in arid soils, the downward soil-water movement in the top meter of the profile is predominantly in the vapor phase. The liquid flux is upward above a null point some 0.20 to 0.35 meters below the land surface in response to capillary pressure gradients brought about by the evaporative demand. Therefore, in the upper portion of the profile, water may be moving downward during summer months (in the vapor phase), while solutes are moving upward (in the liquid phase). This phenomenon has been investigated previously by Rose (1968) through conventional numerical modeling techniques. Thus, a separation in volatile versus conservative solute tracer movement would be expected. The radio-isotope tracer results of Phillips et al. (1988) support this assumption, based upon the distribution of bomb-pulse ^{36}Cl and ^{3}H in the soil profile. A conceptual model of soil-water movement, as influenced under prevailing summer conditions, is presented in Figure 23.

The liquid and vapor flux distributions with depth should be seasonally variable due to changes in precipitation and temperature. Data presented in Figures 17 and 18 show the effect of changing climatic conditions between the August 4 and October 27 samplings. Precipitation during this three month period has both infiltrated into and evaporated from the soil. A sample of water from one precipitation event in Socorro was analyzed during this period, on August 23, 1988.

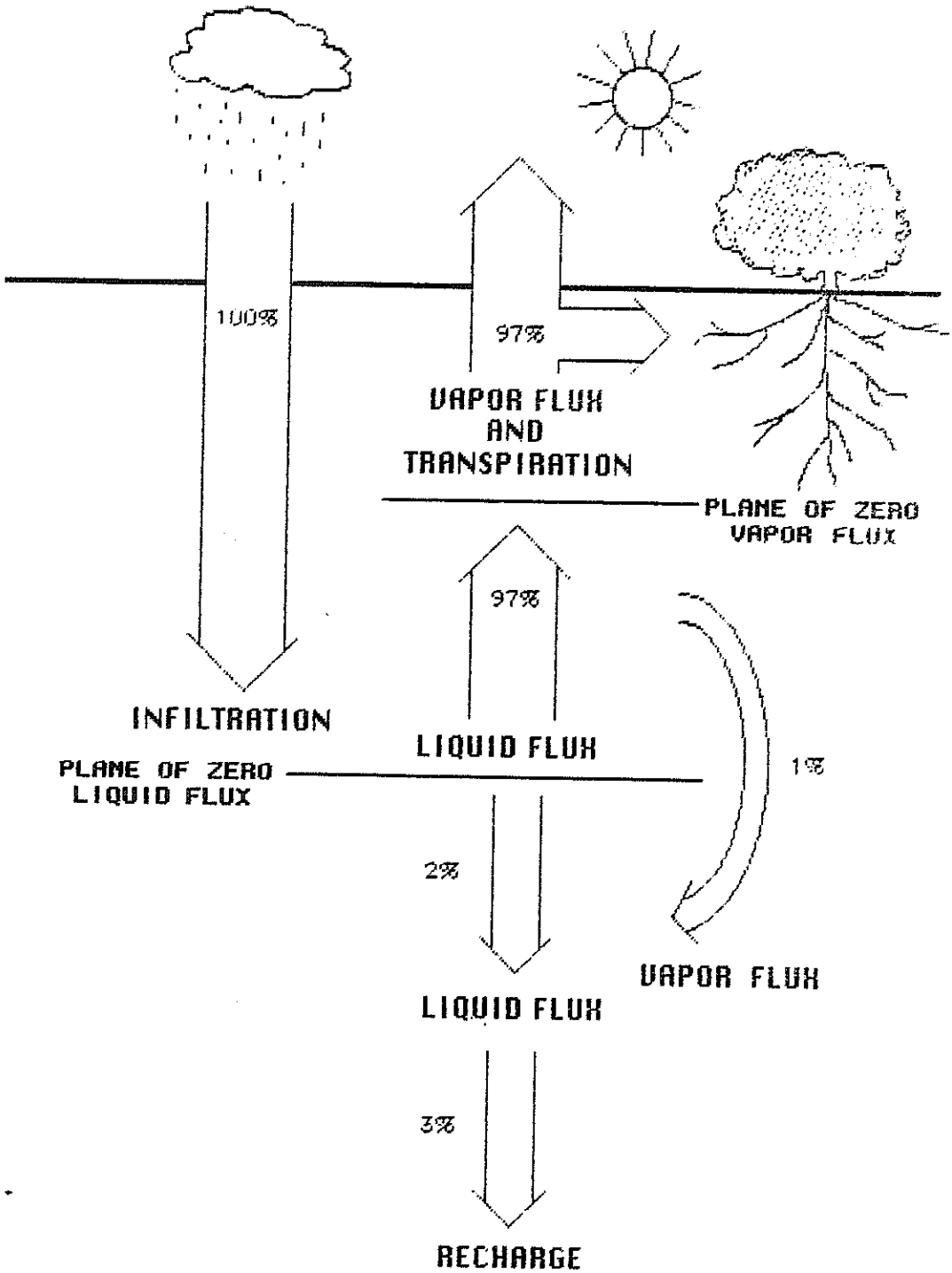

Figure 23. Conceptual depiction of soil-moisture movement under summer conditions. The plane of zero vapor flux occurs approximately 0.12 m below land surface, and the plane of zero liquid flux at 0.20 to 0.35 m.

The δ^2H isotopic composition was $-70^o/_{oo}$. It is evident from Figure 18 that the precipitation during this period has infiltrated and mixed with soil water of enriched composition from the previously developed evaporation zone. Also, residual water is probably displaced ahead of the advancing wetting front. Figure 17 shows that the profile has been wetted to a depth of approximately 1 meter between August 4 and October 27. Figure 18 verifies that the isotopic composition of the soil water has also changed within this depth interval during the same time frame, verifying the mixing process. The added soil moisture will redistribute in the profile, both upwards due to capillary pressure gradients stemming from evaporation at the soil surface, and downwards due to gravity drainage. Uptake of soil water by plant transpiration should also alter the soil moisture regime. These results imply that during seasons of the year other than summer, different mechanisms may be important in the transport of soil water.

The ^{36}Cl profile presented in Figure 1 has a distribution which is worthy of discussion. At the land surface, the $^{36}Cl/Cl$ ratio is at a maximum. Just above a 1 meter depth there is an elevated ratio, or peak. The data below this lower peak exhibits a relatively uniform decrease down to a depth of 3.5 meters. The distribution of ^{36}Cl is therefore markedly different than the tritium distribution, with its broad peak between 2 and 3 meters depth. A similar distribu-

tion of both ^{36}Cl and ^{3}H was presented by Phillips et al. (1988) for a site in southern New Mexico, near Las Cruces. In addition, Figure 24 presents a plot of depth versus $^{36}Cl/Cl$ for a site in Gnome, New Mexico (F.M.Phillips, written communication, January 1989). The same characteristic profile is exhibited in this plot, as at the other two sites mentioned. Namely, there is a maximum ratio at the top of the profile, and an elevated ratio at around one meter in depth. All three sites are located in arid environments. This distribution of ^{36}Cl with depth implies that there is a very complicated history of soil water movement at each site.

The compilation of data just presented leads to some interesting conclusions. During periods of high precipitation enough water may infiltrate into the soil to significantly increase the soil-moisture storage in the top meter of the profile, and undoubtedly transport solutes to depth. Subsequent redistribution of soil water causes the solutes to move both upward and downward in the profile. A maximum $^{36}Cl/Cl$ is maintained at the soil surface, and an elevated level is observed at about one meter depth. During the spring and early summer months the precipitation is small compared with the evapotranspiration demand. The soil water profile develops into a quasi-steady state condition by mid-summer. The downward vapor flux movement of soil water in the top meter of the profile causes water to be trans-

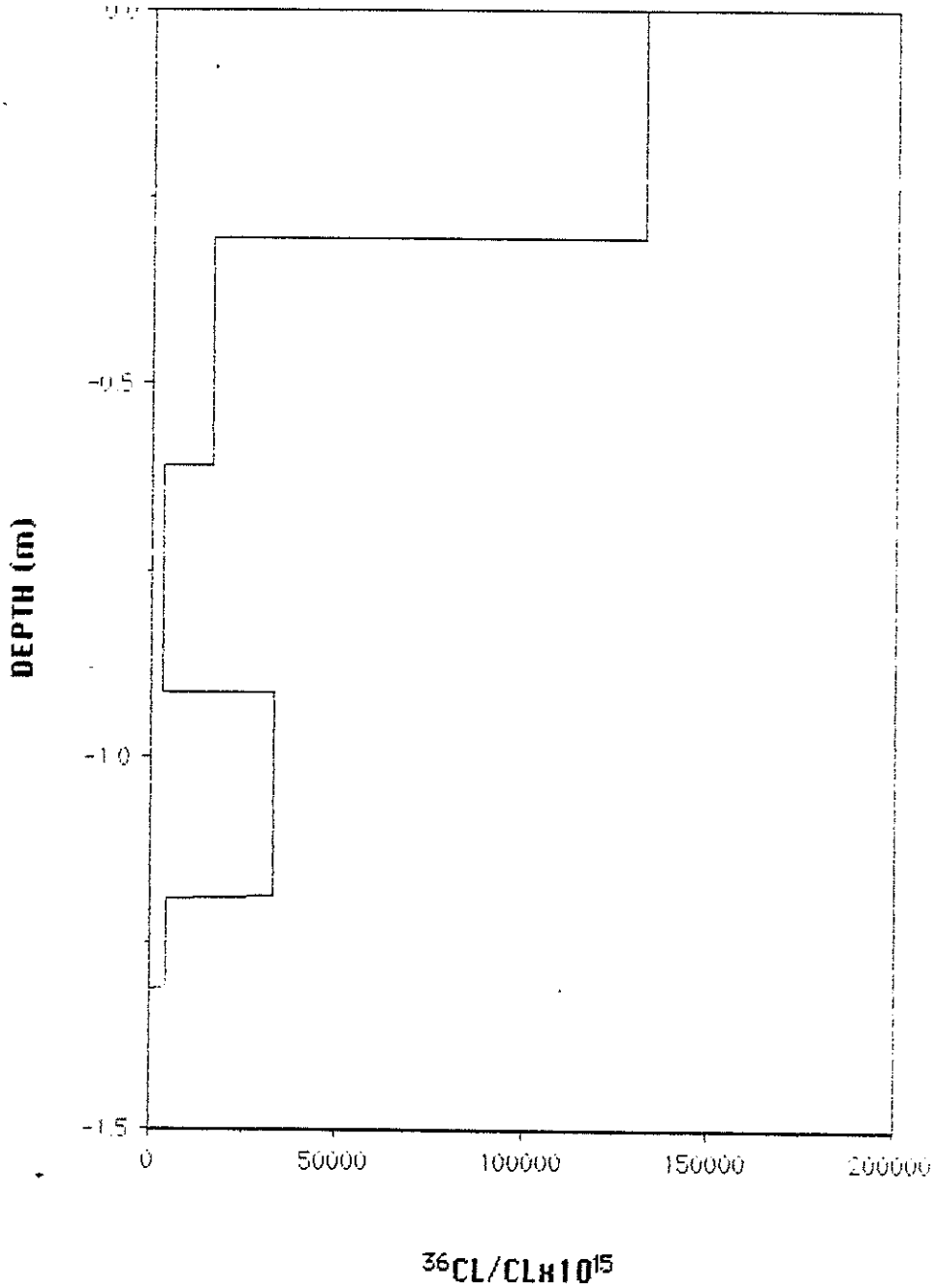

Figure 24. Depth versus $^{36}Cl/Cl$ for a site in Gnome, New Mexico

ported to depth while solutes are moving upward toward the dry surface layer in response to capillary pressure gradients. The entire process is controlled by highly complicated and episodic (diurnal and longer) forcing. The vapor flux portion of soil water movement cannot be ignored in any rigorous treatment of unsaturated flow under natural arid conditions.

Another factor related to the shape of the isotope profiles in the SSIP5 core is the influence of the water table. In Figure 13 it is evident that the ^{18}O and ^{2}H profiles deviate relative to each other between the 2.70 meter depth and the bottom of the profile. The bottom of the profile is very near the present water table elevation. This displacement implies that the ^{18}O-^{2}H relationship is changing due to factors different from those influencing the upper portion of the profile. Figure 14 depicts the ^{2}H versus ^{18}O relationship. The data from above 2.7 meters in depth plot on a straight line with a slope of 3.3, indicative of evaporation through an unsaturated soil profile. The data for the deeper depths are shown as deviating from this trend toward the meteoric water line. This deviation is attributed to a mixing of isotopic compositions between the areal recharge water infiltrating through the profile from the land surface and the water table at depth. The water table elevation at the site varies in response to stream induced recharge along the reach of the Rio Salado. Therefore the

isotopic composition of the ground water influences the composition within the unsaturated portion of the profile. This water table influence is also shown in Figure 1 for the tritium data. Bomb-pulse levels of tritium occur below a depth of 3.5 meters. Just above the 3.5 meter depth, tritium is at background levels. The elevated levels of tritium at depth are an artifact of the changing water table and capillary fringe elevations (Phillips et al. 1988).

The shapes of the SSIP5 profiles in Figures 11 through 13 imply certain qualitative information about the distribution of liquid and vapor fluxes. The maximum enriched value of the isotopic species in the upper 12 cm of the profile is indicative of the evaporation front. The depth of this evaporation front corresponds to a plane of zero flux for water vapor movement at the time this profile was sampled. The flux of water above this depth is predominantly in the vapor phase, i.e., the liquid flux is essentially negligible. This portion of the profile is generally very dry (very low liquid moisture content). The unsaturated hydraulic conductivity of the porous media at these low water contents is very small, and hence negligible when there are long time intervals between precipitation events. The vapor flux in this upper region is upward in response to the lower atmospheric humidity.

Below the plane of zero vapor flux the vapor movement is downward. Several factors contribute to this downward vapor

transport process. Two of these mechanisms are a concentration gradient of the isotopic species, and a thermal gradient, which in turn influences the vapor pressure gradient. Under quasi-steady state conditions with no appreciable temperature influence an exponentially decaying isotopic profile would develop due to concentration driven diffusion (Allison et al. 1984). If, however, a strong temperature gradient exists, there should be a minimum in the profile. Figure 16 shows the depth versus deuterium profiles for the SSIP5 and SSIP6 cores. The minimum in the SSIP5 and SSIP6 isotope profiles is indicative of a strong downward vapor flux within the zone of 0.12 to 1.25 meters depth. The lighter isotopes of water, ^{16}O and H, are condensing out at the deeper portion of this zone, and therefore decreasing the ratios of $^{18}O/^{16}O$ and $^{2}H/H$. A minimum in the isotope profile is a result of strong a temperature gradient (and therefore vapor pressure gradient) which enhances the effect of the concentration-driven diffusive process mentioned previously.

A determination of the slope of the isotope data in Figure 14 can indicate a relative evaporation effect. Performing a linear regression on these data yields the following relationship: $\delta D = 3.30(\delta^{18}O) - 54.5$; where $R^2=0.95$. A δD versus $\delta^{18}O$ slope of 5.0 would be representative of evaporation from a free water surface. A slope of 2.0 or less would be observed if there were a very thick laminar layer associated with the vapor flux region of

evaporation. The data for SSIP5 fall in between these two extremes, as expected. Several techniques (Barnes and Allison 1983) can be used to quantify the evaporation rate from stable isotope profile data.

The estimation of the recharge flux was 0.083 cm/yr, from stable isotope data with the 'piston displacement/mixing' model of Allison et al. (1984). Phillips et al. (1988) have estimated the recharge flux to be 0.84 cm/yr using tritium as a 20 year tracer. Stephens and Knowlton (1986) calculated the recharge rate at 0.70 cm/yr using soil physics techniques. The estimate of 0.083 cm/yr from the PD/M model is one order of magnitude smaller than the other reported recharge rates.

The difference in the predicted recharge rates is attributed to a violation of the governing assumptions in the PD/M technique. The main assumption in the PD/M model is that the recharge flux occurs due to piston displacement of infiltrating soil water. This causes the displacement from the meteoric water line. If different mechanisms control the recharge flux, then this technique would be invalid. Because the recharge rate is considered to be on the order of 0.84 cm/yr, but the deuterium displacement is large enough to be indicative of a low recharge rate, then piston displacement is probably not the main mechanism affecting recharge. This conclusion implies that the vapor flux component of recharge may be important, and thus invalidates the use of

the PD/M model for calculating recharge at this site.

The subject of spatial variability can also be addressed with the existing data. Figure 15 depicted the moisture content distribution for the SSIP5 and SSIP6 cores, collected 70 cm apart on the same day. There is considerable variation with depth between these two profiles. This implies that there are textural differences between the two sampling sites. The isotopic data presented in Figure 16 for the same two cores are lacking in any appreciable variation, however. The uniformity in the isotope profiles implies that the slight textural differences have little to do with isotopic changes. Allison and Hughes (1983) discuss the issue of replication, and conclude that errors associated with limited tracer data may not be as serious as expected. In addition, Foster and Smith-Carrington (1980) sampled six tritium profiles over a sizeable area and found very good lateral uniformity. Therefore we assume that these profiles, although collected at only two points, are representative of soil moisture movement over a larger area.

PRINCIPAL FINDINGS, CONCLUSIONS, AND RECOMMENDATIONS

The stable isotope data obtained in this study have been used to model quantitatively the vapor phase transport of soil moisture as a proportion of deep recharge. Qualitatively, the isotope information has also been used to draw conclusions about the relative importance of the downward vapor flux.

A model was presented which predicts the shape of the isotope profile and the vapor flux portion of recharge under quasi-steady one-dimensional non-isothermal flow conditions. The equation describing the relative shape of the isotope profile was used to fit parameters to a known isotope profile by means of a non-linear least-squares analysis. The parameters determined from this fitting procedure were then used in a model to quantify the vapor flux portion of soil-water movement that eventually becomes recharge. The depth-averaged vapor flux between 0.12 and 2.70 meters depth ranged from 15 to 33 percent of the deep flux, or recharge rate. During the summer months, there was a potential for solutes to travel upward within the top meter of the profile, due to capillary pressure gradients resulting from evaporation at the land surface. Also, water movement was downward, due to a strong vapor flux in response to downward vapor

pressure gradients. This leads to a potential separation of volatile versus conservative solute tracer movement. This idea is consistent with the conclusions drawn by Phillips et al. (1988) in their work with radioisotopes at this same site. The magnitude of the vapor flux is such that it plays a major role in solute transport in the system. The vapor flux is of a sufficient size to influence the total recharge flux. Therefore, the vapor phase flux should be accounted for when determining recharge in water resources planning or hazardous waste siting analyses. However, the vapor flux portion of soil-water movement is important in the summer months, but during the other seasons of the year liquid-phase infiltration and redistribution are probably dominant processes.

Qualitatively, the stable isotope profiles support the conclusion that the vapor flux is appreciable (but the liquid flux dominates) in the recharge process. The presence of the minimum in the isotope profiles from SSIP5 is the basis for making this statement. There is a strong diffusive transport of lighter isotopes downward below the evaporation front, where the lighter isotopes are condensed out to form the minimum in the profile around one meter in depth (Figure 13).

In addition to the vapor flux estimates, a new laboratory distillation technique has been developed during the course of this study. This new vacuum distillation technique

is an alternative to the azeotropic toluene distillation procedure used to extract soil water from soil samples without isotopic fractionation.

The work presented here should prove very useful to scientists, engineers, and water resource planners. The role of vapor phase water movement in the recharge process appears to be very important. It is important from both a water resources planning perspective, and a solute transport perspective. For the water resource planner, the amount of recharge calculated for a given area may be appreciably larger when taking into account the vapor flux component. Also, the transport of volatile contaminants in the vadose zone may be greatly enhanced due to vapor phase flow, whereas non-volatile constituents only travel within the liquid phase at a slower rate. This could be very important in hazardous waste siting.

Additional work on this topic might include such areas as: a more rigorous treatment of the numerical modeling approach, from both a theoretical and practical viewpoint; a transient analysis of the isotope profiles, including seasonal effects in arid environments; and further study into the effects of tortuosity on the liquid and vapor flux components of recharge.

SUMMARY

We present a model which can predict the shape of the stable isotope profiles in the vadose zone, and also quantify the vapor flux portion of soil-water movement that leads to recharge. Through a non-linear least-squares approach, the model is matched to an observed isotope profile by optimizing the values of specified variables. The fitted parameters are then used to solve numerically for the vapor flux as a percentage of the deep flux of water, or recharge. This technique of modeling the isotope species transport is much more robust than conventional heat and moisture flow modeling techniques. This conclusion stems from the fact that the effective diffusivities vary little with water content in the former analysis as compared with the latter.

A depth-averaged estimate of 15 to 33 percent of the soil-water movement in the upper 2.7 meters of the soil profile is comprised of a vapor-phase flux during summer months. The liquid-flux component of recharge is, therefore, the dominant transport mechanism. However, the vapor flux is sufficient enough to influence strongly the solute transport characteristics of the system. This result is consistent with conclusions made by Phillips et al. (1988). A qualitative analysis of the isotope profiles also confirms this

conclusion. The development of an isotope minimum at depth in the profile is indicative of a strong downward vapor flux. This minimum in the profile is a result of the condensation of the lighter isotope species.

A new vacuum distillation technique was developed during this project. This new procedure is an alternative to the azeotropic toluene distillation technique employed in extracting soil water from soil samples without isotopic fractionation.

REFERENCES

Allison, G.B. 1982. The relationship between ^{18}O and deuterium in water in sand columns undergoing evaporation. Journal of Hydrology. 55:163-169.

Allison, G.B., C.J.Barnes, and M.W.Hughes 1983. The distribution of deuterium and ^{18}O in dry soils: 2. Experimental. Journal of Hydrology. 64:377-397.

Allison, G.B., C.J.Barnes, M.W.Hughes, and F.W.J.Leaney 1984. The effect of climate and vegetation on oxygen-18 and deuterium profiles in soils. Isotope Hydrology 1983. IAEA, Vienna, 105-124.

Allison, G.B., and M.W.Hughes 1983. The use of natural tracers as indicators of soil-water movement in a temperate semi-arid region. Journal of Hydrology. 60:157-173.

Allison, G.B., W.J.Stone, and M.W.Hughes 1985. Recharge in karst and dune elements of a semi-arid landscape as indicated by natural isotopes and chloride. Journal of Hydrology. 76:1-26.

Barnes, C.J., and G.B.Allison 1983. The distribution of D and ^{18}O in dry soils: 1. Theory. Journal of Hydrology. 60:141-156.

Barnes, C.J., and G.B.Allison 1984. The distribution of deuterium and ^{18}O in dry soils: 3. Theory for non-isothermal water movement. Journal of Hydrology. 74:119-136.

Bath, A.H., W.G.Darline, and A.P.Brunsdon 1982. The stable isotope composition of infiltration moisture in the unsaturated zone of the English Chalk. Stable Isotopes, Proc. Fourth Inter. Conf., Julich, 23-26 March 1981 (Schmidt, H.-L., Forstel, H., and Heinzinger, K., eds.), Anal. Chem. Symp. Ser., Vol. II, Elsevier, Amsterdam, p. 161-166.

Bergstrom, R.E., and R.E.Aten 1965. Natural recharge and localization of fresh water in Kuwait. Journal of Hydrology. 2:213-231.

Dansgaard, W. 1964. Stable isotopes in precipitation. Tellus. 16:436-468.

Dincer, T., A.Al-Mugrin, and U.Zimmerman 1974. Study of the infiltration and recharge through the sand dunes in arid zones, with special reference to the stable isotopes and thermonuclear tritium. Journal of Hydrology. 23:79-109.

Epstein, S., and T.Mayeda 1953. Variation of ^{18}O content of waters from natural sources. Geochim. Cosmochim. Acta. 4:213-224.

Falconer, K.L., L.C.Hull, and S.A.Mizell 1982. A mathematical model for evaluating the suitability of a low-level radioactive waste site. In Waste Management '82 (Post, R.G., ed.), Vol. 2, Proc. Symp., Tucson, Arizona, 8-11 March 1982, p.245-258.

Foster, S.S.D., and A.Smith-Carrington 1980. The interpretation of tritium in the Chalk unsaturated zone. Journal of Hydrology. 46:343-364.

Grismer, M.E., D.B.McWhorter, and A.Klute 1986. Determination of diffusivity and hydraulic conductivity in soils at low water contents from nondestructive transient flow observations. Soil Science. 141(1):10-19.

Jaynes, D.B. and A.S.Rogowski 1983. Applicability of Fick's law to gas diffusion. Soil Science Society of America Journal. 47:425-430.

Kendall, C., and T.B.Coplen 1985. Multisample conversion of water to hydrogen by zinc for stable isotope determination. Anal. Chem.. June 1985, p.1437-1446.

Kirk-Othmer 1983. Encyclopedia of Chemical Technology. 23:246-273. New York: John Wiley & Sons.

Machette, M.N. 1978. Geologic map of the San Acacia quadrangle, Socorro County, New Mexico. U.S. Geological Survey, Geologic Quadrangle Map GQ-1415.

Majoube, M. 1971. Fractionnement en oxygene 18 et en deuterium entre l'eau et sa vapeur. J. Chim. Phys. 68:1423-1436.

Mann, J.F., Jr. 1976. Waste waters in the vadose zone of arid regions: Hydrologic interactions. Ground Water. 14:367-372.

Mattick, J.L., F.M.Phillips, and T.A.Duval. 1986. Quantification of ground-water recharge rates in New Mexico using bomb-36Cl and bomb-3H as soil-water tracers, New Mexico Water Resources Research Institute Technical Completion Report No. 220, New Mexico State University, Las Cruces, New Mexico.

Merlivat, L. 1979. Molecular diffusivities of $H_2{}^{16}O$, $HD^{16}O$ and $H_2{}^{18}O$ in gases. Journal Chem. Physics. 69:2864-2871.

Mills, R. 1973. Self diffusion in normal and heavy water in the range 1-45°C. Journal Chem. Physics. 77:685-688.

Philip, J.R. and D.A.de Vries 1957. Moisture movement in porous materials under temperature gradients. Trans. Am. Geophys. Union. 38:222-232.

Phillips, F.M., J.L.Mattick, and T.A.Duval 1988. Chlorine-36 and tritium from nuclear-weapons fallout as tracers for long-term liquid and vapor movement in desert soils. Water Resources Research. 24:1877-1891.

Phillips, F.M., K.N.Trotman, H.W.Bentley, and S.N.Davis 1983. ^{36}Cl, an environmental tracer for soil water. Proc. Natl. Conf. Adv. Infil. American Society of Agricultural Engineers, 12-13 December, Chicago.

Phillips, F.M., K.N.Trotman, H.W.Bentley, and S.N.Davis 1984. The bomb-^{36}Cl pulse as a tracer for soil-water movement near Socorro, New Mexico. Selected Papers on Water Quality and Pollution in New Mexico (Stone, W.B., ed.), New Mexico Bureau of Mines and Mineral Resources, Hydrologic Report 7, p.271-280.

Roether, W. 1970. Water-CO_2 exchange set-up for the routine ^{18}oxygen assay of natural waters. International Journal of Applied Radiation and Isotopes. 21:379-387.

Rose, C.W. 1968. Water transport in soil with a daily temperature wave. II. Analysis. Australian Journal of Soil Research. 6:45-47.

Saxena, R.K. 1984. Seasonal variations of oxygen-18 in soil moisture and estimation of recharge in esker and moraine formations. Nordic Hydrology. 15:235-242.

Stephens, D.B. and R.G.Knowlton, Jr. 1986. Soil-water movement and recharge through sand at a semi-arid site in New Mexico. Water Resources Research. 22:881-889.

Stephens, D.B., R.G.Knowlton, Jr., J.McCord, and W.Cox 1985. Field study of natural ground water recharge in a semi arid lowland. New Mexico Water Resources Research Institute Technical Completion Report No. 177, New Mexico State University, Las Cruces, New Mexico.

Stone, W.J., and B.E.McGurk 1985. Ground-water recharge on the southern High Plains, east-central New Mexico. New Mexico Geological Society Guidebook, 36th Field Conference, Santa Rosa, p.331-336.

Taylor, S.A., and J.W.Carey 1964. Linear equations for the simultaneous flow of matter and energy in a continuous soil system. Soil Science Society of America Proceedings. 28:167-172.

Thoma, G., N.Esser, C.Sonntag, W.Weiss, J.Rudolph, and P.Leveque 1979. New techniques of in-situ soil moisture sampling for environmental isotope analysis applied at Pilat sand dune near Bordeaux. Isotope Hydrology, Proceedings of the International Symposium. 1978, IAEA, 2:753-768.

U.S. Department of Agriculture 1972. New Mexico water resources: assessment for planning purposes. 22 maps, Soil Conservation Service.

Vuataz, F.D., and F.Goff 1986. Isotope geochemistry of thermal and nonthermal waters in the Valles Caldera, Jemez Mountains, northern New Mexico. Journal of Geophysical Research. 91:1835-1854.

Verhagen, B.Th., P.E.Smith, I.McGeorge, and Z.Dziembowski 1979. Tritium profiles in Kalahari sands as a measure of rain-water recharge. Isotope Hydrology, Proceedings of the International Symposium. 1978, IAEA, 2:733-751.

Weast, R.C. 1975. Handbook of Chemistry and Physics. Edited by R.C.Weast, 55th ed., Cleveland, Ohio: Chemical Rubber Company.

Zimmerman, U., D.Enhalt, and K.O.Munnich 1967. Soil-water movement and evapotranspiration: Changes in the isotopic composition of the water. Isotopes in Hydrology, 1966, Proceedings of the IAEA Symposium, Vienna, p.567-584.

APPENDIX A

Field and Laboratory Data

Field and Laboratory Data

Sevilleta Stable Isotope Profile 3

Depth (m)	δ^2H (permil)	$\delta^{18}O$ (permil)	Water Content (cc/cc)	Temperature (^oC)
-0.075	-50.0	-4.6	0.078	22.2
-0.225	-68.0	-2.7	0.087	19.6
-0.375	-60.1	-4.3	0.075	18.7
-0.525	-61.0	-7.0	0.059	18.4
-0.675	-67.7		0.043	18.2
-0.825	-66.0	-3.3	0.043	18.9
-1.200	-62.7	-7.4	0.034	19.4
-1.525	-72.8	-7.0	0.039	18.7
-1.840		1.5	0.035	18.1
-2.225	-56.6	-6.0	0.040	17.7
-2.465		-2.7	0.053	19.1
-2.735	-70.0	5.3	0.034	17.9
-2.970	-62.4	-5.6	0.053	17.9
-3.275	-65.0	2.0	0.039	18.5
-3.640	-60.0	-6.7	0.036	17.9
-3.970	-64.7	-8.0	0.336	18.8
-4.220	-63.1	-6.8	0.137	18.3
-4.375	-66.0	-5.5	0.055	19.0

Field and Laboratory Data

Sevilleta Stable Isotope Profile 4

Depth (m)	δ^2H (permil)	$\delta^{18}O$ (permil)	Water Content (cc/cc)	Temperature (^oC)
-0.013	-49.6	1.6	0.011	28.7
-0.043	-40.0	6.5	0.013	26.9
-0.205	-57.0	0.2	0.031	26.1
-0.285	-54.4	0.2	0.039	27.4
-0.380	-45.2	2.5	0.037	26.6
-0.480	-76.8	-6.0	0.039	26.8
-0.585	-74.4	-7.9	0.034	25.7
-0.695	-80.6	-8.7	0.037	25.5
-0.805	-63.5	-4.4	0.041	24.2
-1.200	-74.6	-7.9	0.030	22.4
-1.390	-40.6	-1.7	0.038	21.7
-1.585	-80.9	-7.1	0.033	22.3
-1.800	-73.6	-4.7	0.033	20.4
-2.085	-61.6	-3.6	0.041	22.9
-2.365	-76.3	-4.9	0.098	20.2
-2.955	-59.9	-2.9	0.054	22.3
-3.495	-70.8	-7.0	0.038	22.7
-3.980	-73.6	-7.1	0.254	20.1
-4.185	-64.2	-6.1	0.171	18.8
-4.405	-64.5	-5.8	0.071	22.8
-4.655	-59.8	-5.7	0.067	20.9
-4.945	-62.5	-6.6	0.077	20.5

Field and Laboratory Data

Sevilleta Stable Isotope Profile 5

Depth (m)	δ^2H (permil)	$\delta^{18}O$ (permil)	Water Content (cc/cc)	Temperature (^oC)
-0.013	-29.7	7.9	0.016	
-0.038	-17.2	10.3	0.026	
-0.070	-17.4	9.2	0.027	
-0.115	-34.2	7.4	0.024	
-0.170	-40.5	5.0	0.024	28.4
-0.225	-44.5	4.0	0.027	28.4
-0.300	-54.2	1.3	0.032	30.0
-0.400	-67.2	-3.4	0.029	30.1
-0.500	-70.6	-4.4	0.032	30.4
-0.590	-77.7	-5.6	0.035	30.5
-0.680	-77.7	-6.7	0.032	30.0
-0.775	-82.8	-7.4	0.044	30.8
-0.860	-84.6	-8.1	0.032	29.9
-0.950	-86.0	-8.7	0.033	30.0
-1.050	-88.6	-9.5	0.032	
-1.140	-87.0	-9.1	0.033	30.0
-1.320	-87.5	-9.5	0.038	28.5
-1.520	-83.9	-8.8	0.036	29.1
-1.705	-83.3	-8.2	0.034	27.9
-1.900	-86.2	-8.4	0.037	23.2
-2.100	-83.8	-7.7	0.041	
-2.300	-83.8	-7.6	0.053	28.0
-2.500	-79.5	-6.9	0.037	29.0
-2.700	-81.0	-7.4	0.034	25.8
-2.880	-76.2	-7.5	0.054	25.5
-3.125	-71.8	-6.8	0.041	
-3.290	-71.2	-6.1	0.042	25.6
-3.505	-71.6	-6.2	0.039	24.9
-3.740	-72.8	-6.4	0.038	24.3
-4.240	-69.3	-7.3	0.057	23.9
-4.450	-68.7	-7.5	0.058	23.6
-4.535	-67.5	-7.6	0.058	23.4

Field and Laboratory Data

Sevilleta Stable Isotope Profile 6

Depth (m)	δ^2H (permil)	$\delta^{18}O$ (permil)	Water Content (cc/cc)	Temperature (^oC)
-0.020	-19.1		0.017	
-0.060	-10.9		0.048	
-0.105	-29.0		0.025	
-0.165	-37.3		0.026	
-0.230	-44.2		0.030	
-0.300	-55.3		0.030	
-0.380	-61.7		0.030	
-0.460	-70.3		0.030	
-0.540	-65.5		0.030	
-0.620	-80.5		0.034	
-0.840	-76.3		0.030	
-1.040	-84.5		0.044	
-1.220	-88.4		0.052	
-1.500	-81.0		0.034	
-2.020	-79.9		0.034	
-2.310	-81.3		0.041	
-2.530	-73.8		0.040	
-2.800	-67.0		0.044	
-3.070	-62.4		0.040	
-3.330	-67.9		0.047	

Field and Laboratory Data

Sevilleta Stable Isotope Profile 7

Depth (m)	δ^2H (permil)	$\delta^{18}O$ (permil)	Water Content (cc/cc)	Temperature (^oC)
-0.010	-86.4		0.012	
-0.033	-59.3		0.015	
-0.053	-47.4		0.016	
-0.073	-50.3		0.020	
-0.098	-43.9		0.026	
-0.125	-45.7		0.041	
-0.155	-51.1		0.047	
-0.185	-60.1		0.051	
-0.250	-62.0		0.058	
-0.335	-66.4		0.063	
-0.395	-63.3		0.060	
-0.470	-62.3		0.074	
-0.570	-62.2		0.070	
-0.670	-63.0		0.086	
-0.785	-64.9		0.081	
-0.900	-66.1		0.085	
-1.000	-76.4		0.073	
-1.110	-81.7		0.058	
-1.220	-85.1		0.033	
-1.325	-84.7		0.041	
-1.535	-83.7		0.035	
-1.945	-81.9		0.038	
-2.150	-80.3		0.037	